Contribution from the Laboratoire d'Electrochimie de l'Université de Paris 7, Unité Associée au CNRS No. 438, 75 251 Paris Cedex 05, France, and Institut Curie, Section de Biologie, Unité INSERM 219, Centre Universitaire, 81405 Orsay, France

Molecular Environment Effects in Redox and Coordination Chemistry. Protection against Solvation, Local Solvation, and Steric Hindrance to Ligation in the Electrochemistry of Basket-Handle Iron Porphyrins

Claire Gueutin,[1a] Doris Lexa,[1a] Michel Momenteau,[1b] Jean-Michel Savéant,*[1a] and Feng Xu[1a]

Received June 17, 1986

The thermodynamics of the four reactions $Fe^{II} + Cl^- \rightleftarrows Fe^{II}Cl^-$, $Fe^{II} + e^- \rightleftarrows Fe^{I-}$, $Fe^{I-} + e^- \rightleftarrows Fe^{"0"\,2-}$, and $Fe^{III}Cl + e^- \rightleftarrows Fe^{II}Cl^-$ and the kinetics of the first are investigated, by means of cyclic voltammetry and spectroelectrochemistry, in the five solvents dimethylformamide, *N*-methylacetamide, benzonitrile, *n*-butyronitrile, and 1,2-dichloroethane as a function of the nature and spatial arrangement of the chains in a series of four ether-linked basket-handle porphyrins, four amide-linked basket-handle porphyrins, and one picket-fence porphyrin. The observed influence of the chains, from comparison with the unprotected tetraphenyl- and tetra-*o*-anisylporphyrins, is quite large. It is shown to result from the combination of three effects: protection against external solvation by steric hindrance of the approach of the solvent molecules; "local solvation" by secondary amide groups included in the chain; steric discrimination between axial ligands. The magnitude of these effects is estimated and shown to depend upon the nature, bulkiness, and flexibility of the chains and the nature of the solvent. This illustrates the more general concept of how relatively simple molecular superstructures can be used to modulate the reactivity of a central molecule without participating directly to the reaction, in a manner that is reminiscent of the modulation of the reactivity of the prosthetic group by the microenvironment offered by the protein chains in metalloproteins.

The remarkable efficiency, smoothness, and selectivity of the chemistry carried out by enzymatic systems is presumably related to their structure involving a central reacting center, the prosthetic group, surrounded by protein chains that offer a microenvironment able to modulate its reactivity without participating directly to the reaction. The idea of supramolecular chemistry and electrochemistry derives from attempts to imitate, even remotely, theses structures and their functions.

In this connection we discuss in the following the possibility of modifying the reactivity of a central reactant by relatively simple carbon chain superstructures, choosing as an example the redox and coordination reactivity of iron porphyrins as reacting centers. These molecules offer the advantage of exhibiting chemical properties that are relevant to aromatic organic, coordination, and organometallic chemistry. The influence of the superstructures on their reactivity is thus likely to be a good model for the modulation of the reactivity of molecules belonging to various different areas of chemistry. On the other hand, iron porphyrins serve as prosthetic groups in several natural metalloproteins (hemoglobin, myoglobin, cytochromes, cytochrome oxidases).

The superstructured porphyrins investigated in the present work are, with the exception of one of them, of the "basket-handle" type (Figures 1 and 2). They derive from tetraphenylporphyrin by attaching two basket-handle carbon chains to the ortho positions of the phenyl rings. As shown in the following, the mode of attachment, ether linkage (Figure 1) or secondary amide linkage (Figure 2) has a cruxial importance in the modifications of the reactivity of the central porphyrin complex. In each series, three porphyrins contain two 12-carbon-atom aliphatic chains (14 chain links). They differ by the spacial arrangement of the chains, cross-trans, adjacent-trans, and adjacent-cis. In both the ether-linked and amide-linked series, a fourth porphyrin contains two C_4–Ph–C_4 chains in a cross-trans configuration. We have also added to the amide-linked series the Collman's picket-fence porphyrin[2b] (Figure 2). These molecules belong to a vast family of superstructured porphyrins that have been synthetized during the past decade in the aim of mimicking particular functions of the surrounding protein chains in several natural metalloproteins.[2]

In the work described hereafter, we examine the influence of the superstructures shown in Figures 1 and 2 on the reactivity of the iron porphyrin complex in a series of four redox or coordination reactions that all involve the creation of a negative charge in the complex:

$$Fe^{II} + Cl^- \rightleftarrows Fe^{II}Cl^- \qquad (1)^3$$

$$Fe^{II} + e^- \rightleftarrows Fe^{I-} \qquad (2)^{3,4,6}$$

$$Fe^{I-} + e^- \rightleftarrows Fe^{"0"\,2-} \qquad (3)^{5,6}$$

$$Fe^{III}Cl + e^- \rightleftarrows Fe^{II}Cl^- \qquad (4)$$

The thermodynamics, standard potentials or equilibrium constants, were investigated in all four cases and the kinetics in one case, reaction 1, by using as a source of information the cyclic voltammetry and spectroelectrochemistry of the iron(III) complexes.

As will be demonstrated in the following, the superstructures exert three types of effects in the series of reactions: protection against external solvation by steric hindrance of the approach of the solvent molecules; "local solvation" by secondary amide groups included in the chains; steric discrimination between axially bound ligands including coordinating solvent molecules. In order to unravel this superposition of effects, the above reactions were investigated in five different solvents, dimethylformamide (DMF), *N*-methylacetamide (NMA), benzonitrile (PhCN), *n*-butyronitrile

(1) (a) Université de Paris 7. (b) Institut Curie.

(2) (a) For reviews on the purposes and syntheses of superstructured porphyrins see ref 2b–h. (b) Collman, J. P. *Acc. Chem. Res.* **1977**, *10*, 265. (c) Jones, R. D.; Summerville, D. A.; Basolo, F. *Chem. Rev.* **1979**, *79*, 139. (d) Smith, P. D.; James, B. R.; Dolphin, D. H. *Coord. Chem. Rev.* **1981**, *39*, 31. (e) Traylor, T. G. *Acc. Chem.* Res. **1981**, *14*, 102. (f) Bogatskii, A. V.; Zhilina, Z. I. *Russ. Chem. Rev. (Engl. Transl.)* **1982**, *51*, 592. (g) Collman, J. P.; Halpert, T. R.; Suslick, K. S. *Metal Ion Activation of Dioxygen*; Spiro, T. G.; Ed., Wiley: New York, 1980; pp 1–72. (h) Baldwin, J. E.; Perlmutter, P. *Top. Curr. Chem.* **1984**, *121*, 181. (i) Dolphin, D. H., manuscript in preparation.

(3) The iron(II) complex on the left-hand side actually bears solvent molecules as axial ligands in coordinating solvents.

(4) (a) There is good spectroscopic[4b–h] and chemical[4i] evidence that the dominant resonance form is a Fe(I) complex rather than a Fe(II) porphyrin anion radical. (b) Cohen, I. A.; Ostfeld, D.; Lichtenstein, B. *J. Am. Chem. Soc.* **1972**, *74*, 4522. (c) Lexa, D.; Momenteau, M.; Mispelter, M. *Biochim. Biophys. Acta* **1974**, *338*, 151. (d) Kadish, K. M.; Larson, G.; Lexa, D.; Momenteau, M. *J. Am. Chem. Soc.* **1975**, *97*, 282. (e) Reed, C. A. *Adv. Chem. Ser.* **1982**, *No. 201*, 333. (f) Mashiko, T.; Reed, C. A.; Haller, K. J.; Scheidt, W. R. *Inorg. Chem.* **1984**, *23*, 3192. (g) Srivatsa, G. S.; Sawyer, D. T.; Boldt, N. J.; Bocian, D. F. *Inorg. Chem.* **1985**, *24*, 2123. (h) Hickman, D. L.; Shirazi, A.; Goff, H. M. *Inorg. Chem.* **1985**, *24*, 563. (i) Lexa, D.; Mispelter, J.; Savéant, J. M. *J. Am. Chem. Soc.* **1981**, *103*, 6806.

(5) Although the evidence is not as strong as for Fe(I),[4] the most likely dominant resonance form of the Fe("0") complex appears to be an Fe(I) porphyrin anion radical.[4h] For the sake of simplicity we will however keep on with the formal notation Fe("0").

(6) Fe(I) and Fe("0") do not bear axial ligands, at least at room temperature.[4]

0020-1669/86/1325-4294$01.50/0

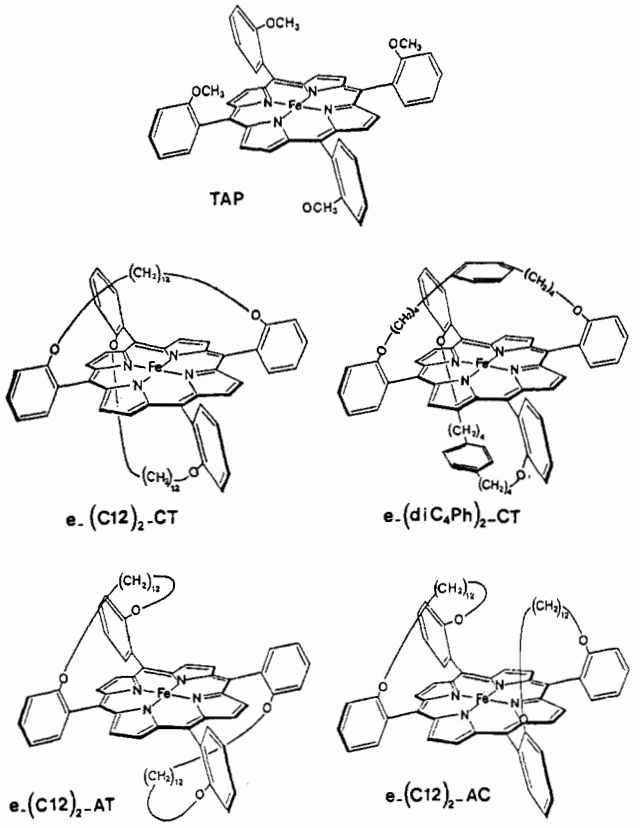

Figure 1. Tetra-*o*-anisylporphyrin (TAP) and ether-linked basket-handle porphrins investigated in this work. In the conventional designation given below each porphyrin, e stands for "ether-linked" and AC, AT, and CT are abbreviations describing the arrangement of the two chains: adjacent-cis, adjacent-trans, and cross-trans, respectively.

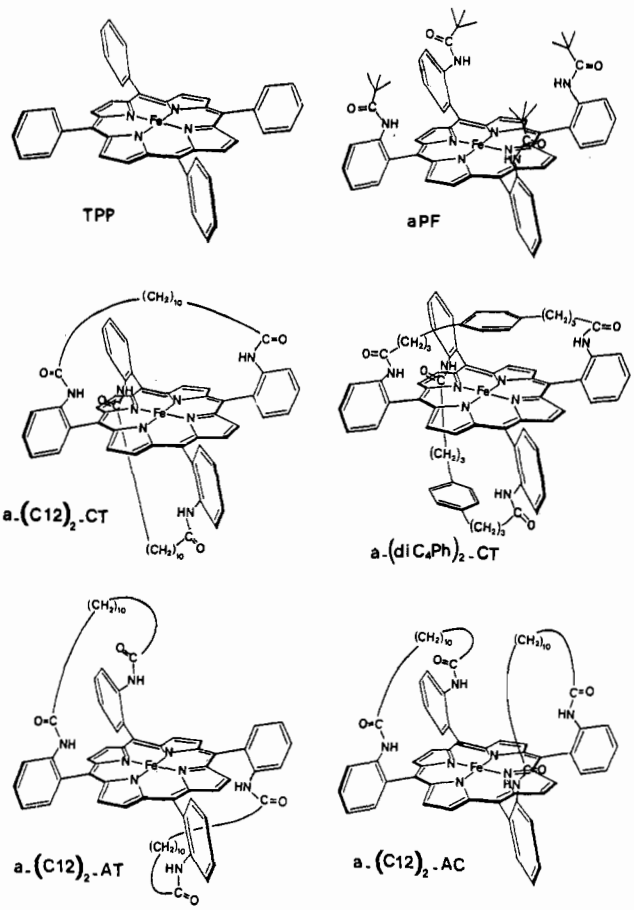

Figure 2. Tetraphenylporphyrin (TPP) and picket-fence (a-PF) and amide-linked basket-handle porphyrins investigated in this work. a stands for "amide-linked". The other abbreviations are the same as in Figure 1.

(PrCN), and 1,2-dichloroethane (DCE). The solvent can indeed play two opposite roles. As a Lewis acid, it is able to solvate the negatively charged species. As a Lewis base, it is involved in the axial coordination of the iron(II) complexes.[6] It is thus expected that the chains not only protect the central complex against solvation at the Fe^{I} and Fe^{0} $^{2-}$ oxidation states but may also sterically interact with the axially bound solvent molecules in the Fe(II) complex. The choice of DCE, a very poor Lewis base, was made for eliminating the latter factor, hence simplifying the analysis of the external and internal solvation effects. Unfortunately DCE, like alkyl monohalides, reacts with both Fe(I)[4i] and Fe("0").[8d] Reaction with iron("0") is quite fast within the time scale of cyclic voltammetry, thus precluding the investigation of reaction 3 in this solvent. Reaction of DCE with iron(I) is sufficiently slow for allowing the cyclic voltammetric characterization of reaction 2. PrCN, PhCN, and DMF are increasingly good axial ligands of iron(II) while having comparable acceptor properties.[7] They allow the investigation of all four reactions. As discussed below, PhCN differs from PrCN in the sense that it may give rise to $\pi-\pi$ electronic interactions. NMA, which has a complexing power similar to that of DMF,[7a] was selected because it is a very strong solvating agent of anions,[7b] due to the fact that it contains a secondary amide group. It was thus of interest to use this solvent in relation to the local solvent effect taking place in the amide-linked superstructured porphyrins. The anion-solvating power of NMA is actually so strong that the iron(II) porphyrins are practically not coordinated by Cl^- ions in NMA whatever the porphyrin structure in the investigated series. The study was thus restricted to reactions 2 and 3 in this solvent. Nevertheless, NMA is a solvent of particular interest for two reasons. Due to its very strong anion-solvating power, it allows to test the strength of the steric protection offered by the basket-handle superstructures. On the other hand, it contains a secondary amide group, as do the protecting chains in the amide-linked basket-handle or picket-fence porphyrins.

In a preliminary investigation carried out in DMF as the solvent we have examined the influence of the C12 basket-handle superstructures on reactions 1–3 and concluded the existence of the three aforementioned effects.[8a,9,10] Similar effects have also been

(7) (a) The Gutman donor numbers are respectively 26.6 (DMF), 15.1 (PhCN), and 16.1 (PrCN).[7c] NMA is likely to have a donor number close to that of DMF.[7d] DCE is such a poor Lewis base that it is usually selected as the reference solvent for defining the donor numbers of the other solvents.[7c] (b) The Gutman acceptor numbers are 16 (DMF),[7e] ca. 30 (NMA),[7f] 15.5 (PhCN),[7e] ca. 15 (PrCN),[7f] and 16.7 (DCE).[7g] (c) Gutman, V. *The Donor-Acceptor Approach to Molecular Interactions*; Plenum: New York, 1978; p 20. (d) From the comparison between DMF (26.6),[7g] dimethylacetamide (27.8),[7g] and formamide (24).[7g] (e) Reference 7c, p 29. (f) Values interpolated from the linear relationship existing between the Gutman acceptor number[7e,g] and the Reichardt parameter[7h] for several solvents (hexamethylphosphorotriamide, dimethylacetamide, DMF, acetonitrile, dimethylsulfoxide, *N*-methylformamide, formamide). (h) Reichardt, C. *Angew. Chem., Int. Ed. Engl.* **1979**, *18*, 98. (g) Mayer, V. *Stud. Phys. Theor. Chem.* **1983**, *27*, 219.

(8) (a) Lexa, D.; Momenteau, M.; Rentien, P.; Rytz, G.; Savéant, J. M.; Xu, F. *J. Am. Chem. Soc.* **1984**, *106*, 4755. (b) Lexa, D.; Momenteau, M.; Savéant, J. M.; Xu, F. *Inorg. Chem.* **1985**, *24*, 122. (c) Croisy, A.; Lexa, D.; Momenteau, M.; Savéant, J. M. *Organometallics* **1985**, *4*, 1574. (d) Lexa, D.; Savéant, J. M.; Wang, D. L. *Organometallics* **1986**, *5*, 1428.

(9) Sparse data were also previously gained in benzonitrile with the e-$(C12)_2$-CT and a-$(C12)_2$-CT iron porphyrins.[8a,b]

(10) (a) Another electrochemical study of superstructured porphyrins has dealt with short straps containing solely carbon atoms.[10b] The observed effects on the redox properties of the free bases and of the zinc and magnesium complexes were rationalized in terms of distortion of the porphyrin ring caused by the shortness of the straps. The effects we discuss here are of quite different nature since the basket handles are of sufficient length to not induce such constraints. (b) Becker, J. Y.; Dolphin, D.; Paine, J. B.; Wijesekera, T. *J. Electroanal. Chem. Interfacial Electrochem.* **1984**, *164*, 335.

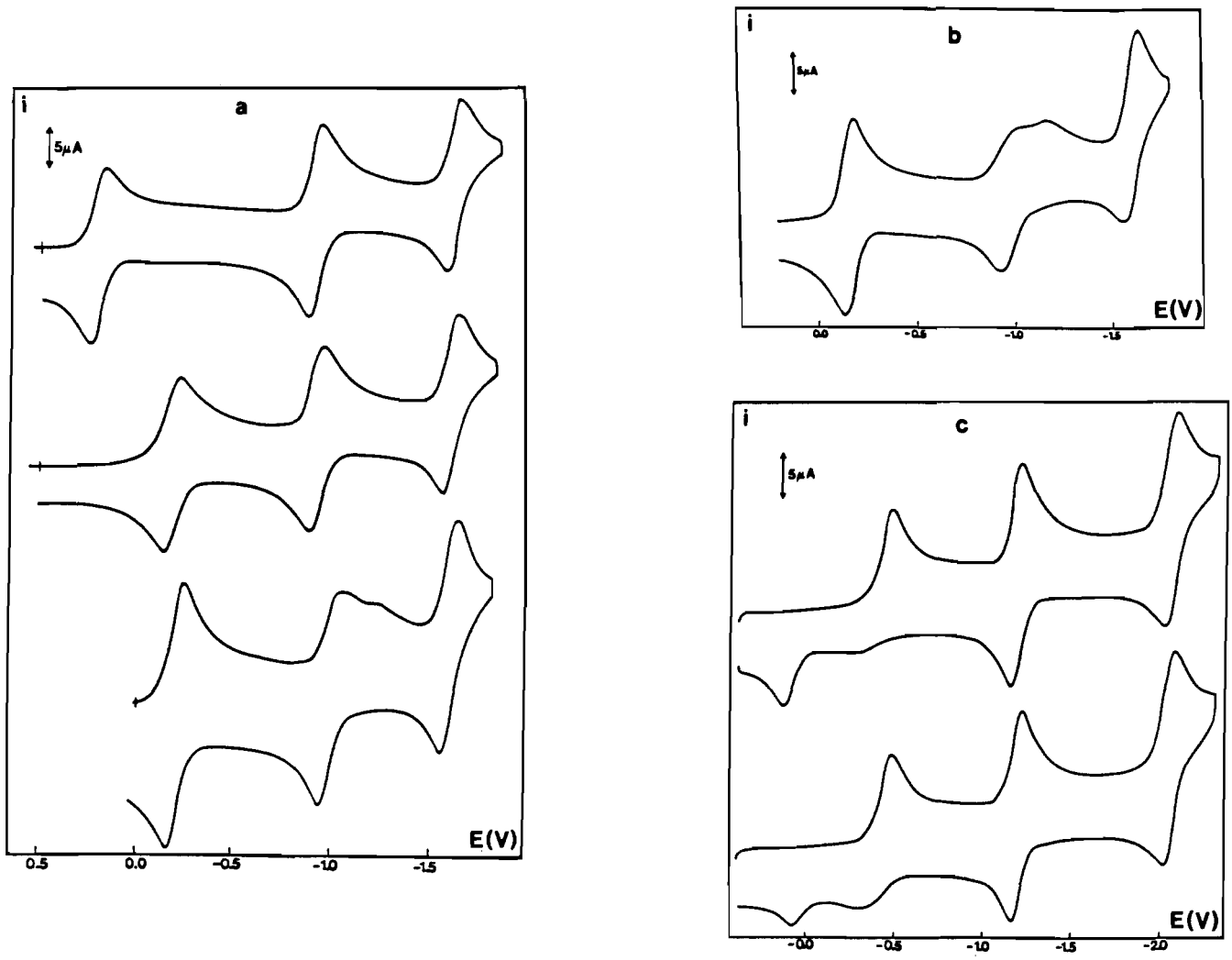

Figure 3. Typical examples of the variations of the cyclic voltammograms upon addition of Cl^- ions in PrCN (+0.1 M NBu_4ClO_4): (a) a-$(diC_4Ph)_2$-CT-Fe^{III} (from top to bottom) OH^- complex neutralized by an equimolar amount of $HClO_4$, after addition of 1 mM Cl^-, after addition of 12 mM Cl^-; (b) a-$(C12)_2$-AT-$Fe^{III}Cl$; (c) e-$(diC4Ph)_2$-CT-$Fe^{III}Cl$ (from top to bottom) without further addition of Cl^-, in the presence of 10 mM Cl^-. Sweep rate: 0.1 $V \cdot s^{-1}$. Temperature: 20 °C. Porphyrin concentration: 1 mM.

qualitatively shown to influence the complexation of iron(II) by hydroxide ions[8b] and the addition of carbon monoxide to iron(I) porphyrins.[8c] The purpose of the present work was, by investigating more reactions and using a larger number of solvents and of superstructured porphyrins, to better identify the various effects exerted by the chains and to estimate their magnitudes.

Results

In order to obtain quantities featuring the specific effect of the chains on the reactivity of the iron porphyrin center, we systematically compared the ether-linked basket-handle porphyrins to tetra-*o*-anisylporphyrin (TAP) and the amide-linked basket-handle and picket-fence porphyrins to TPP. As further elaborated in the Discussion, this allows one to eliminate with a good approximation the electronic inductive effect of the anchoring groups at the ortho position of the phenyl rings.

Cyclic voltammetry was the main technique we employed for characterizing reactions 1–4. It was supplemented by thin-layer spectroelectrochemistry for the determination of the association equilibrium constant of reaction 1 in several instances.

Figure 3 shows typical examples of the cyclic voltammetry of the investigated porphyrins in one of the solvents, PrCN. Three wave systems are observed, featuring successively, from left to right, the reduction of Fe(III) into Fe(II), Fe(II) into Fe(I), and Fe(I) into (Fe"0"). The same general behavior is observed for all porphyrins in all solvents except with DCE, where only the first two steps are visible.

It is seen that, provided the water content of the solvent is low enough, the last cathodic wave, featuring the $Fe^{I-}/Fe^{"0"\,2-}$ couple, is reversible. The same was observed for all porphyrins in all solvents with the exception of DCE. This behavior is expected from the fact that neither Fe(I) nor Fe("0") bear any axial ligand at room temperature. A quite straightforward *determination of the standard potential of the* $Fe^{I-}/Fe^{"0"\,2-}$ *couple* as the midpoint between the cathodic and anodic peaks ensues. The results thus obtained are listed in Table I.

The first two cathodic–anodic wave systems are more complicated, depending upon the amount of Cl^- ion present in the solution, the nature of the porphyrins, and the solvent.

Figure 3a shows the results obtained with a-$(diC4Ph)_2$-CT in PrCN. In the absence of Cl^- ions, the two first waves are reversible, corresponding to the reduction of PrCN complexes of Fe(III) and Fe(II). Upon addition of millimolar amounts of Cl^- the first wave undergoes a large negative potential shift and the second a small negative potential shift. This indicates that both the Fe(III) and Fe(II) complexes bind Cl^- as an axial ligand, Fe(III) to a larger extent than Fe(II). Both waves however remain reversible. Upon addition of more Cl^- ions the second cathodic wave splits into two waves. The first of them decreases at the expense of the second and becomes S shaped as the Cl^- concentration and/or the sweep rate are raised. This behavior has already been observed in DMF, for example with TPP.[8a,11] It corresponds to the oxido reductions of Scheme I. Fe(III) is strongly complexed

(11) (a) Bottomley, L. A.; Kadish, K. M. *Inorg. Chem.* **1981**, *20*, 1348. (b) Lexa, D.; Rentien, P.; Savéant, J. M.; Xu, F. *J. Electroanal. Chem. Interfacial Electrochem.* **1985**, *191*, 253.

Scheme I

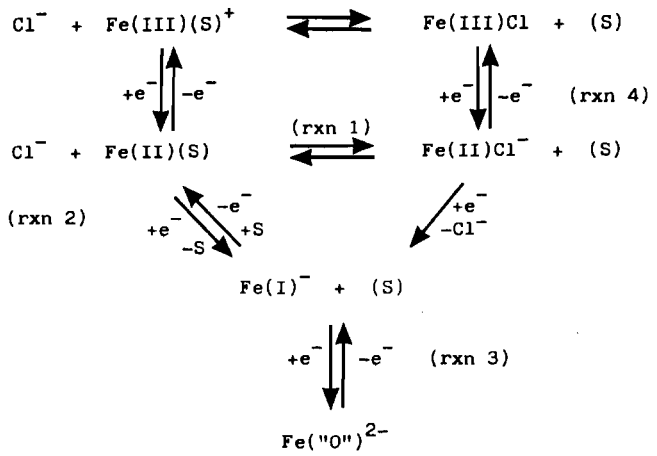

by Cl^-[8a,b,11b] and exists practically only under this form. $Fe^{II}Cl^-$ is easier to oxidize and more difficult to reduce than $Fe^{II}S$. Thus, both the reduction and the oxidation of Fe(II) occur along "CE" mechanisms.[12] They are however opposite one another: in reduction, the conversion of $Fe^{II}Cl^-$ into $Fe^{II}S$ precedes the first electron transfer ($Fe^{II}S$ being easier to reduce than $Fe^{II}Cl^-$), whereas in oxidation, the converse reaction precedes the first electron transfer ($Fe^{II}Cl^-$ being easier to oxidize than $Fe^{II}S$). In the particular case of the a-$(diC_4Ph)_2$-CT porphyrin in PrCN, $Fe^{II}Cl^-$ predominates over $Fe^{II}S$ at equilibrium even in the presence of a millimolar concentration of Cl^-. Thus, the oxidation of Fe(II) gives rise to a single wave, corresponding to fast equilibrium, at Cl^- concentrations of both 1 and 10 mM. This is also the case for the reduction with $[Cl^-] = 1$ mM. Upon raising of the Cl^- concentration up to 10 mM, the reduction wave splits into two waves with the first taking a kinetic character, as expected from the shifting of the equilibrium toward $Fe^{II}Cl$.

Parts b and c of Figure 3 illustrate the changes of the cyclic voltammetric patterns when passing from one porphyrin to the other in the same solvent, PrCN in the present case. Figure 3b shows what is observed with a porphyrin, a-$(C12)_2$-AT, for which Fe(II) has a strong affinity for Cl^- ions. It is observed that the cathodic wave featuring the reduction of Fe(II) splits into two waves, with the first having a kinetic character, without adding more Cl^- ions over the stoichiometric concentration (1 mM).

In contrast, Figure 3c shows the cyclic voltammograms obtained with a porphyrin, e-$(diC_4Ph)_2$-CT, for which the affinity toward Cl^- ions is particularly small. It is seen that even in the presence of 10 mM Cl^-, the reduction wave of Fe(II) remains reversible. On the other hand, the oxidation wave of Fe(II) now shows a splitting into two waves. The less positive wave featuring the oxidation of $Fe^{II}Cl^-$ is small, exhibits a kinetic character, and increases upon addition of Cl^-. This indicates that the $Fe^{II} + Cl^- \rightleftarrows Fe^{II}Cl^-$ equilibrium is now in favor of the left-hand side. Reaction 1 has no influence on the reduction of Fe(II) since Fe(II) is easier to reduce than $Fe^{II}Cl^-$. It oppositely and kinetically controls the oxidation of Fe(II) since the small amount of $Fe^{II}Cl^-$ existing at equilibrium is oxidized first, being continuously regenerated by association of Fe(II) and Cl^- as $Fe^{II}Cl^-$ is consumed at the electrode surface.

The reduction wave of Fe(II) and/or its oxidation wave therefore contain information concerning the thermodynamics of reactions 1, 2, and 4 and the kinetics of reaction 1. In order to obtain the values of $E^\circ_{Fe^{II}/Fe^{I}-}$, K_A, k_A, k_D, and $E^\circ_{Fe^{III}Cl/Fe^{II}Cl^-}$, we used complementary or alternative strategies depending mainly upon the magnitude of K_A, which is itself a function of the solvent and of the porphyrin structure. The analysis of the kinetic waves observed in the cyclic voltammetry of either the reduction or the oxidation of iron(II) was based on the theory recently developed for such systems[11b,13b] and illustrated on the example of Fe(TPP)Cl.[11b] It allows the treatment of pseudo-first-order as well as second-order conditions according to the amount of Cl^- ions present in the solution.[11b,13b]

The starting Fe(III) complexes were available as chlorides in all cases and also as hydroxides in some cases.

Several procedures were followed for the determination of the standard potentials of the $Fe^{II}/Fe^{I}-$ couple.

A. In the cases where the association equilibrium constant of Fe(II) with Cl^- was known from spectroelectrochemistry (vide infra), $E^\circ_{Fe^{II}/Fe^{I}-}$ could be determined from the cyclic voltammetry experiments carried out with the $Fe^{III}Cl$ complex without any addition of Cl^- ions. A first subcase is when the $Fe^{II}/Fe^{I}-$ wave is reversible, showing no kinetic character. The standard potential was then derived from the measured cathodic half-peak potential and from the value of K_A determined spectroscopically.[13] The correction from the effect of Fe(II) complexation with Cl^- is negligible when $K_AC^\circ \leq 0.1$ (C° = porphyrin concentration); i.e. for millimolar solutions, $K_A \leq 10^2$ M^{-1}.[13c] Under such conditions, $E^\circ_{Fe^{II}/Fe^{I}-}$ can simply be obtained as the midpoint between the cathodic and anodic peak potentials of the reversible wave (procedure A1), as in the case of the $Fe^{I}-/Fe^{"0"\,2-}$ couple. When K_AC° takes larger values, the correction was carried out as already described[13] (procedure A2). Another subcase arises when, even without addition of Cl^- in excess of the stoichiometric concentration, the reduction wave splits into two waves with the first of them showing a kinetic character. Then, knowing K_A from spectroelectrochemistry, we derived $E^\circ_{Fe^{II}/Fe^{I}-}$, k_A, and k_D from the measurement of the height of the first cathodic wave and that of its half-peak potential (procedure A3).[13]

B. In the case where $K_AC^\circ \leq 0.1$, the reduction wave of Fe(II) in the absence of added Cl^- is reversible and located at the standard potential $E^\circ_{Fe^{II}/Fe^{I}-}$ as discussed above. The equilibrium constant can then be derived from cyclic voltammetric experiments carried out in the presence of excess Cl^-. If the $Fe^{II}/Fe^{I}-$ wave then remains reversible, the midpoint between the cathodic and anodic peak potentials, $E_{1/2}$, is, under these conditions, simply given by

$$E_{1/2} = E^\circ_{Fe^{II}/Fe^{I}-} - (RT/F) \ln (1 + K_A[Cl^-])$$

which, from the measurement of $E_{1/2}$, allows one to determine K_A. If, the $Fe^{II}/Fe^{I}-$ wave splits into two waves with the first having a kinetic character, K_A can still be determined together with k_A and k_D.[13] A related iteration procedure (procedure B1) can be used in the case where, K_AC° being larger, $E_{1/2}$ of the Fe(II) reduction wave is not exactly equal to $E^\circ_{Fe^{II}/Fe^{I}-}$.[13d]

C. When the iron(III) porphyrin was available in the form of a hydroxide, $E^\circ_{Fe^{II}/Fe^{I}-}$ could be determined as the midpoint of the reversible wave obtained upon neutralization by a solution of concentrated perchloric acid in the considered solvent.[8b] This procedure (procedure C1) was found to be applicable in the cases of DMF, PhCN, and PrCN. In the case of DCE the stock acid solution must be made with another solvent, which has the drawback of introducing the latter in the solution. Its concentration is however not very high, of the order of 100 times the porphyrin concentration. An alternative method that starts from

(12) (a) A chemical reaction, here a ligation or a ligand-exchange reaction, precedes the electron-transfer step.[12b] (b) Savéant, J. M.; Vianello, E. *Electrochim. Acta* **1963**, *8*, 905.

(13) (a) All these procedures are described in details elsewhere.[13b] (b) Savéant, J. M.; Xu, F. *J. Electroanal. Chem. Interfacial Electrochem.* **1986**, *208*, 197. (c) In the reversible case, it appears that when $K_AC^\circ \leq 0.1$, the half-wave potential is only 2 mV (at 20 °C) negative to the value that would be obtained in the absence of Cl^- ions. Correction of the potentials from the effect of Cl^- complexations then becomes negligible. (d) The method consists of taking as starting value of $E^\circ_{Fe^{II}/Fe^{I}-}$ the $E_{1/2}$ obtained from the reversible $Fe^{II}/Fe^{I}-$ wave in the absence of added Cl^-. This is then used to extract from the experiments in the presence of excess Cl^- the value of K_A. This latter value is then used to obtain a second value of $E^\circ_{Fe^{II}/Fe^{I}-}$ from the experiment without Cl^- added. This new value of $E^\circ_{Fe^{II}/Fe^{I}-}$ is then used to extract a new value of K_A from the experiments with excess of Cl^- and so forth, until $E^\circ_{Fe^{II}/Fe^{I}-}$ and K_A become practically constant (we stopped the iteration procedure when E° varied by less than 1 mV). The treatment of the data pertaining to excess Cl^- is carried out by using either eq 1 when the corresponding $Fe^{II}/Fe^{I}-$ wave remained reversible or a procedure already described[13a,b] when it was split into two waves with the first one having kinetic character.

Table I. Thermodynamic and Kinetic Data

Solvent [f] (temperature)	Porphyrin	$E^\circ_{Fe(I)^-/Fe("0")^{2-}}$ [a,b,c]	$E^\circ_{Fe(II)/Fe(I)^-}$ [a,c,e]		K_A (M^{-1}) [d,e]			k_A ($M^{-1}.s^{-1}$) [e]		k_D (s^{-1})	$E^\circ_{Fe(III)Cl/Fe(II)}$ [a,c,e]	
DMF [g] (20°C)	TAP	-1.767	-1.058	A1	$3.1\ 10^1$		D1	$7.2\ 10^4$	F3	$2.3\ 10^3$	-0.281	G2
	e-$(C12)_2$-AC	-1.842 (-75)	-1.098 (-40)	"	3.6	(-54)	"	$1.9\ 10^4$	"	$5.2\ 10^3$	-0.365 (-84)	"
	e-$(C12)_2$-AT	-1.862 (-95)	-1.093 (-35)	"	$3.4\ 10^{-1}$	(-114)	"	$5.3\ 10^4$	"	$1.6\ 10^5$	-0.398 (-117)	"
	e-$(C12)_2$-CT	-1.947 (-180)	-1.125 (-67)	"	$6.5\ 10^{-1}$	(-98)	"	$1.9\ 10^3$	"	$2.9\ 10^3$	-0.391 (-110)	"
	e-$(diC_4Ph)_2$-CT	-1.938 (-171)	-1.078 (-29)	"	$9.6\ 10^{-2}$	(-146)	"	$2.9\ 10^2$	"	$3.0\ 10^3$	-0.379 (-98)	"
	TPP	-1.650	-0.984	"	$5.6\ 10^1$		"	$1.0\ 10^5$	F1	$2.0\ 10^3$	-0.191	G2
	a-PF	-1.440 (210)	-0.812 (172)	A2	$3.6\ 10^3$	(105)	"	$6.8\ 10^4$	"	$1.9\ 10^1$	-0.103 (88)	"
	a-$(C12)_2$-AC	-1.455 (195)	-0.850 (134)	"	$1.8\ 10^3$	(88)	"	$4.6\ 10^4$	F5	$2.6\ 10^1$	-0.118 (73)	"
	a-$(C12)_2$-AT	-1.505 (145)	-0.853 (131)	"	$3.0\ 10^3$	(101)	"	$3.8\ 10^4$	F5	$1.2\ 10^1$	-0.074 (117)	"
	a-$(C12)_2$-CT	-1.530 (120)	-0.886 (98)	"	$1.2\ 10^3$	(77)	"	$1.0\ 10^5$	F1,F5	$8.6\ 10^1$	-0.138 (53)	"
	a-$(diC_4Ph)_2$-CT	-1.505 (145)	-0.900 (84)	C1	$1.1\ 10^2$	(17)	E1	$6.8\ 10^3$	"	$6.2\ 10^1$	-0.183 (8)	"
NMA (35°C)	TAP	-1.660	-1.110	A1								
	e-$(C12)_2$-AC	-1.680 (-20)	-1.150 (-40)	"								
	e-$(C12)_2$-AT	-1.695 (-35)	-1.150 (-40)	"	—			—			—	
	e-$(C12)_2$-CT	-1.835 (-175)	-1.200 (-90)	"								
	e-$(diC_4Ph)_2$-CT	-1.855 (-195)	-1.125 (-15)	"								
	TPP	-1.535	-1.085	"								
	a-PF	-1.430 (105)	-0.920 (165)	"								
	a-$(C12)_2$-AC	-1.430 (105)	-0.987 (100)	"								
	a-$(C12)_2$-AT	-1.420 (115)	-0.970 (115)	"	—			—			—	
	a-$(C12)_2$-CT	-1.477 (52)	-0.985 (100)	"								
	a-$(diC_4Ph)_2$-CT	-1.443 (92)	-0.945 (140)	"								
PhCN (20°C)	TAP	-1.734	-1.107	"	$1.3\ 10^2$		D1	$5.6\ 10^3$	F1	$4.3\ 10^1$	-0.386	G2
	e-$(C12)_2$-AC	-1.958 (-224)	-1.195 (-88)	"	8.8	(-68)	"	$4.7\ 10^2$	F3	$5.4\ 10^1$	-0.447 (-61)	"
	e-$(C12)_2$-AT	-1.938 (-204)	-1.195 (-88)	"	3.9	(-89)	"	$6.3\ 10^2$	"	$1.6\ 10^2$	-0.488 (-102)	"
	e-$(C12)_2$-CT	-1.925 (-191)	-1.239 (-132)	C1	2.2	(-103)	D1,E1	$3.3\ 10^2$	"	$1.5\ 10^2$	-0.515 (-119)	"
	e-$(diC_4Ph)_2$-CT	-1.988 (-254)	-1.190 (-83)	A1	$4.4\ 10^{-1}$	(-144)	" ,"	$5.4\ 10^2$	"	$1.3\ 10^3$	-0.475 (-89)	"
	TPP	-1.690	-1.029	A3	$1.8\ 10^2$		D1	$5.4\ 10^3$	F1	$2.9\ 10^1$	-0.322	G2
	a-PF	-1.536 (154)	-0.777 (253)	"	$8.5\ 10^5$	(214)	D2	$1.6\ 10^8$	F2	$2.0\ 10^2$	-0.198 (124)	G1
	a-$(C12)_2$-AC	-1.551 (139)	-0.831 (198)	"	$5.9\ 10^5$	(204)	"	$2.1\ 10^8$	"	$3.6\ 10^2$	-0.179 (143)	"
	a-$(C12)_2$-AT	-1.620 (70)	-0.827 (203)	"	$3.5\ 10^5$	(191)	"	$3.0\ 10^8$	"	$8.7\ 10^2$	-0.181 (141)	"
	a-$(C12)_2$-CT	-1.630 (60)	-0.895 (134)	A3,C1	$2.5\ 10^5$	(183)	D2,E2	$6.5\ 10^8$	"	$2.6\ 10^3$	-0.230 (92)	"
	a-$(diC_4Ph)_2$-CT	-1.540 (150)	-0.924 (105)	A2	$9.8\ 10^2$	(43)	D1	$1.9\ 10^6$	F1	$1.9\ 10^3$	-0.259 (63)	"
PrCN (20°C)	TAP	-1.805	-1.016	A2	$1.0\ 10^3$		D1	$1.3\ 10^6$	F1	$1.3\ 10^3$	-0.393	G2
	e-$(C12)_2$-AC	-1.935 (-130)	-1.183 (-167)	A1	$7.6\ 10^1$	(-65)	"	$4.6\ 10^3$	F4	$6.1\ 10^1$	-0.455 (-62)	G4
	e-$(C12)_2$-AT	-1.940 (-135)	-1.191 (-175)	"	$7.4\ 10^1$	(-66)	"	$2.1\ 10^3$	F4	$2.8\ 10^1$	-0.446 (-53)	G4
	e-$(C12)_2$-CT	-2.065 (-260)	-1.197 (-181)	"	9.7	(-117)	"	$9.0\ 10^2$	F3	$9.0\ 10^1$	-0.494 (-101)	G3
	e-$(diC_4Ph)_2$-CT	-2.030 (-225)	-1.165 (-149)	"	2.0	(-157)	"	$9.4\ 10^2$	F3	$4.7\ 10^2$	-0.477 (-84)	G3
	TPP	-1.682	-1.002	A2	$3.8\ 10^3$		D1	$1.0\ 10^6$	F1	$2.7\ 10^2$	-0.283	G2
	a-$(C12)_2$-AC	-1.546 (136)	-0.871 (131)	C2	$3.0\ 10^5$	(110)	E2	$1.4\ 10^8$	F2	$4.7\ 10^2$	-0.144 (139)	G1
	a-$(C12)_2$-AT	-1.618 (64)	-0.884 (118)	"	$2.0\ 10^5$	(100)	"	$1.1\ 10^8$	"	$5.2\ 10^2$	-0.179 (104)	"
	a-$(C12)_2$-CT	-1.622 (60)	-0.889 (113)	C1	$2.5\ 10^5$	(104)	"	$7.5\ 10^8$	"	$3.0\ 10^3$	-0.206 (77)	"
	a-$(diC_4Ph)_2$-CT	-1.570 (111)	-0.877 (125)	C1,C2	$5.5\ 10^3$	(9)	D1	$7.2\ 10^6$	F1	$1.3\ 10^3$	-0.213 (70)	"
DCE (20°C)	TAP		-1.048	B1	$4.8\ 10^3$		B1	$1.7\ 10^6$	F1	$3.5\ 10^2$	-0.375	G2
	e-$(C12)_2$-AC	—	-1.236 (-188)	B1	$2.0\ 10^2$	(-80)	B1	$1.2\ 10^4$	F3	$6.2\ 10^1$	-0.498 (-123)	"
	e-$(C12)_2$-CT		-1.275 (-227)	A1,C1	$4.5\ 10^1$	(-118)	B2	$7.6\ 10^2$	F3	$1.7\ 10^1$	-0.498 (-121)	"
	TPP		-1.010	B	$7.2\ 10^3$		B1	$1.6\ 10^6$	F1	$2.2\ 10^2$	-0.311	G2
	a-$(C12)_2$-AC	—	-0.886 (124)	B	$1.2\ 10^6$	(129)	D2	$3.7\ 10^8$	F2	$3.1\ 10^2$	-0.232 (79)	G1
	a-$(C12)_2$-CT		-0.879 (131)	C1	$1.0\ 10^6$	(125)	E2	$8.8\ 10^8$	F2	$8.8\ 10^2$	-0.220 (91)	"

a : V vs the NaCl saturated calomel electrode. b : determined as the midpoint between the cathodic and anodic peak potential of the corresponding reversible cyclic voltammetric wave. c : between parenthesis : $E^\circ_{e\text{-}BHP}-E^\circ_{TAP}$ or $E^\circ_{a\text{-}BHP}-E^\circ_{TPP}$ in mV. d : between parenthesis : $(RT/F)Ln(K_A^{e\text{-}BHP}/K_A^{TAP})$ or $(RT/F)Ln(K_A^{a\text{-}BHP}/K_A^{TPP})$. e : conventional numbering of the procedure used for the determination of this quantity as described in the text. f : supporting electrolyte : 0.1 M NBu_4ClO_4 unless otherwise stated. g : supporting electrolyte : 0.1 M $LiClO_4$.

the iron(III) chloride complex is to eliminate the complexation with Cl^- by adding a solution of $AgClO_4$ until Fe^{II}/Fe^{I-} ceases to shift toward positive potentials. This procedure (procedure C2) proved to be effective in PrCN but not in DCE, where the reduction of Ag^+ overlaps with the reduction of the iron(II) porphyrin.

The values of $E°_{Fe^{II}/Fe^{I}}$ obtained by means of these various methods are listed in Table I. Cross-checking of the results obtained for the same system with two independent methods was satisfactory (A3 and C1 for a-$(C12)_2$-CT in PhCN, C1 and C2 for a-$(diC_4Ph)_2$-CT in PrCN). A particular difficulty arose in the case of e-$(C12)_2$-CT in DCE. At 20 °C, the Fe(II)/Fe(I) wave exhibits a definite catalytic character starting from the Fe(III) chloride complex as well as from the neutralized $Fe^{III}OH$ complex. The wave is no longer quite reversible and tends to be S-shaped (Figure 4). The standard reversible Nernstian behavior is restored upon decreasing the temperature (Figure 4). This phenomenon is likely to be caused by the reaction of DCE with Fe(II), followed by further reduction and decomposition, regenerating the Fe(III) complex as observed and discussed in the case of aliphatic monohalides.[8d] That this occurs with the e-$(C12)_2$-CT porphyrin to a larger extent than with the others is related to the fact that the $E°$ of the Fe(II)/Fe(I) couple is then the most negative in the series (Table I). It was found that the $E_{1/2}$ (midpoint between the cathodic and anodic peak potentials) is a linear function of the absolute temperature (Figure 4e). Since within this narrow range of temperature the enthalpy and entropy of the overall reaction (including the reference electrode) are not expected to vary appreciably, this shows that the $E_{1/2}$ measured at 20 °C is not significantly affected by the catalytic process.[14] It can thus be taken as a reliable value of $E°_{Fe^{II}/Fe^{I}}$ in the case of the neutralized hydroxy complex. That this value is not appreciably affected by the presence of the 30 mM of PhCN introduced in the solution upon neutralization is shown by the fact that, at −2 °C, the $E_{1/2}$ values are the same when the neutralized OH^- complex or directly the chloro complex is used. In the latter case, $E_{1/2}$ is practically equal to $E°$ in view of the small value of K_A. We likewise neglected the effect of the introduction of a small amount of PhCN in the determination of $E°_{Fe^{II}/Fe^{I}}$ by procedure C1 in the case of a-$(C12)_2$-CT in DCE.

The various procedures used for the *determination of the Fe(II) chloride association equilibrium constant*, K_A, were as follows.

D. Thin-layer spectroelectrochemistry,[15] setting the electrode potential slightly negative to the Fe^{III}/Fe^{II} reduction potential, was used in most cases. When K_A is not too large, i.e., smaller than about 10^4 M^{-1}, it can be obtained from experiments where chloride ions are progressively added to the solution starting with concentrations that are at least 10 times the porphyrin concentration (procedure D1). One or the other of the two equations

$$\frac{1}{D - D_0} = \frac{1}{D_\infty - D_0}\frac{1}{K_A[Cl^-]} + \frac{1}{D_\infty - D_0}$$

$$\frac{1}{D - D_\infty} = \frac{1}{D_0 - D_\infty}K_A[Cl^-] + \frac{1}{D_0 - D_\infty}$$

are then used according to the magnitude of K_A (D is the observed absorbance, D_0 the absorbance of Fe(II), and D_∞ that of $Fe^{II}Cl^-$). For small K_A's, D_0 is readily obtained from the spectrum in the absence of Cl^-, whereas D_∞ cannot be reached in the available range of Cl^- concentrations and thus use is made of the first equation. The opposite is true for large K_A's, and thus the second equation is used. Either the Soret band or the visible bands or both can be employed for this titration of Fe(II) by chloride ions.

The range of availability of K_A can be extended up to about 10^6 M^{-1} by using a dilution procedure (procedure D2). No Cl^- is added into the solution over the stoichiometric amount introduced with the iron(III) complex. Dissociation of the $Fe^{II}Cl^-$ complex is then obtained by decreasing the concentration of the starting $Fe^{III}Cl$ complex.[8b]

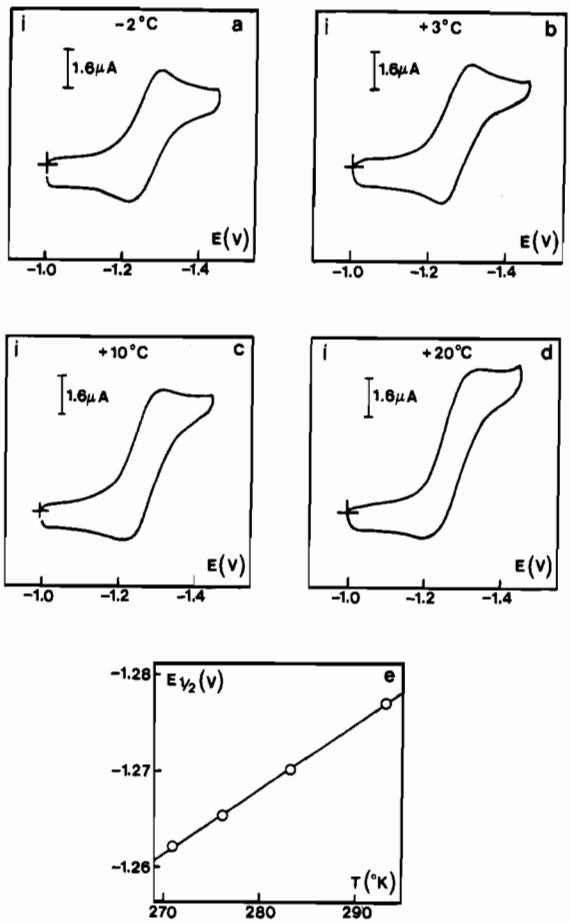

Figure 4. Cyclic voltammetry of e-$(C12)_2$-CT–Fe^{III} (0.5 mM) in DCE (+0.1 M NBu_4ClO_4 + 50 mM PhCN from the neutralization of the $Fe^{III}OH$ complex by a PhCN perchloric acid solution) as a function of temperature: (a) −2 °C; (b) 3 °C; (c) 10 °C; (d) 20 °C; (e) variation of the half-wave potential (midpoint between the cathodic and anodic peak potentials) with the absolute temperature. Sweep rate: 0.1 $V·s^{-1}$.

In DMF, PhCN, and PrCN the Fe(II) complex in the absence of chloride ions is expected to be axially ligated by solvent molecules whereas the solvent should not interfere in the case of DCE. K_A should thus be regarded as the equilibrium constant for the replacement of one solvent molecule by Cl^- in most cases. Different results were however obtained with ether-linked basket-handle porphyrins in PrCN. Parts a and b of Figure 5 compare the spectra obtained in the Soret region of e-$(diC_4Ph)_2$-CT and a-$(diC_4Ph)_2$-CT, respectively. In the second case, a single peak located at 432 nm is observed whereas in the first the Soret band in split into three peaks, the central one being also located at 432 nm. This suggests that Fe(II) is axially complexed by one solvent molecule in the second case, whereas in the first, a mixture of axially uncomplexed and complexed Fe(II) species are dealt with. This is confirmed by experiments carried out in DCE, a noncomplexing solvent, with progressive addition of PrCN (Figure 5c). We start with a Soret band of the hyperporphyrin type,[16a] i.e., split into two peaks of similar height, as expected in a noncoordinating solvent.[16b,e] Upon addition of PrCN an intermediate peak, at 432 nm, appears and grows at the expense of the two other peaks. Treatment of these data (Figure 5d) leads to an equilibrium constant for the association of PrCN with the e-$(diC_4Ph)_2$-CT–Fe^{II} porphyrin of 0.13 M^{-1}. Similar results were obtained with the

(14) (a) This is not actually very surprising since in the case where the substrate is in large excess, as here, catalysis results in an increase of the wave height, a loss of reversibility, and a change of the wave shape without a change in the potential location of the wave.[14b-e] (b) Savéant, J. M.; Vianello, E. *Advances in Polarography*, Proceedings of the 2nd International Congress; Pergamon: Oxford, England, 1960; 367. (c) Savéant, J. M.; Vianello, E. *Electrochim. Acta* **1965**, *10*, 905. (d) Andrieux, C. P.; Blocman, C.; Dumas-Bouchiat, J. M.; M'Halla, F.; Savéant, J. M., *J. Electroanal. Chem. Interfacial Electrochem.* **1980**, *113*, 19. (e) Savéant, J. M.; Su, K. B. *J. Electroanal. Chem. Interfacial Electrochem.* **1984**, *171*, 341.

(15) Lexa, D.; Savéant, J. M.; Zickler, J. *J. Am. Chem. Soc.* **1977**, *99*, 2786.

(16) (a) Gouterman, M. In *The Porphyrins*; Dolphin, D., Ed.; Academic: New York, 1978; Vol. III, p 73. (b) A similar spectrum was obtained with TPP in DCE[16c] and benzene[16d] and also with e-$(C12)_2$-CT in toluene.[16e] (c) Kadish, K. M.; Rhodes, R. K. *Inorg. Chem.* **1983**, *22*, 1090. (d) Brault, D.; Rougee, M. *Biochemistry* **1974**, *13*, 4598. (e) Momenteau, M.; Loock, B. *J. Mol. Catal.* **1980**, *7*, 315.

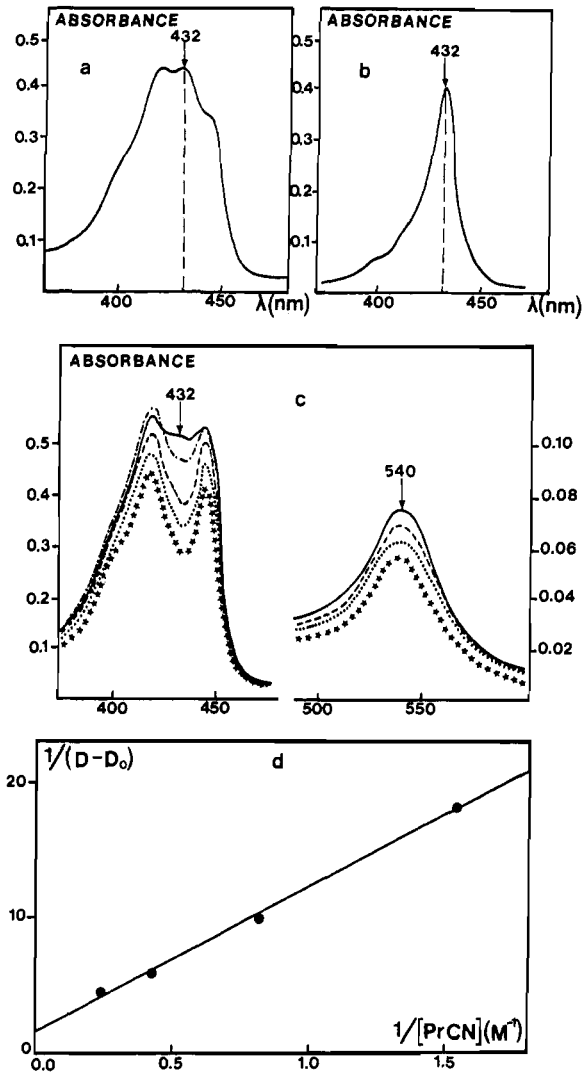

Figure 5. Thin-layer spectroelectrochemistry of e-$(C12)_2$-CT and a-$(C12)_2$-CT-Fe(III). Complexation of Fe(II) by PrCN: (a) e-$(diC_4Ph)_2$-CT (0.1 mM) in pure PrCN; (b) a-$(diC_4Ph)_2$-CT (0.04 mM) in pure PrCN; (c) e-$(diC_4Ph)_2$-CT (0.14 mM) in DCE upon addition of PrCN, from bottom to top 0.00, 0.65, 1.21, 2.30, and 4.07 M PrCN; (d) analysis of the data of Figure 3c at 432 nm according to the equation $1/(D - D_0) = 1/(D_\infty - D_0) + 1/(D_\infty - D_0)\, K_A^{PrCN}[PrCN]$, leading to $K_A^{PrCN} = 0.13\ M^{-1}$. Supporting electrolyte: 0.1 M NBu_4ClO_4. Electrolysis potential: −0.7 V vs. NaCl SCE.

other ether-linked basket-handle porphyrins in PrCN, whereas TAP, TPP, and all the amide-linked porphyrins showed a single Soret peak, indicating that the PrCN axially bound form predominates in the latter series. With the other two coordinating solvents, DMF and PhCN, a simple Soret peak was found with the ether-linked basket-handle porphyrins as well as with the others, showing that the major Fe(II) complex in solutions of these solvents bears a solvent molecule as axial ligand.

E. K_A could also be determined from cyclic voltammetric data by using the neutralization procedures described before (procedures C1 and C2) for determining $E°_{Fe^{II}/Fe^{I-}}$. Once $E°$ is obtained, K_A can be derived from the cyclic voltammetric data obtained with excess chloride ions. Equation 1 was used in this connection when the value of Fe^{II}/Fe^{I-} thus obtained was reversible whereas the method described in ref 13b was used in the case of a kinetic wave. We denote E1 and E2 these procedures according to amount of Cl^- present in the solution, excess or stoichiometric, respectively.

The iteration procedure described earlier (procedure B1) that provides both $E°_{Fe^{II}/Fe^{I-}}$ and K_A was also employed in several cases. A related but different procedure was used in the particular case of e-$(C12)_2$-CT in DCE. Addition of Cl^- considerably increases the catalytic character of the Fe^{II}/Fe^{I-} wave, as expected from the resulting negative shift of the reduction potential. The resulting cyclic voltammograms cannot therefore be used to obtain K_A according to procedure B1. A similar procedure but one applied to the Fe(II)/Fe(III) oxidation wave (procedure B2) was used instead. Upon introduction of a large amount of Cl^- (0.26 M) the Fe(II)/Fe(III) wave is reversible whereas in the presence of a small concentration of Cl^- (6.8 mM for a porphyrin concentration of 0.3 mM) two oxidation waves are seen with the first having a kinetic character. The same iteration procedure as for the Fe^{II}/Fe^{I-} system then allows one to derive K_A, k_A, k_D, and in addition, $E°$ of the $Fe^{III}Cl/Fe^{II}Cl^-$ couple.

The results obtained by applying these various methods are listed in Table I. Again, when two different procedures were used, the results were practically the same.

The case of NMA is worth particular comment. With, e.g., TPP it was observed that both the Fe(III)/Fe(II) and Fe^{II}/Fe^{I-} waves remain reversible with no change of their location in potential upon addition of 0.1 M Cl^- ions. This shows that the association constant of Cl^- is less than about 1 M^{-1} in both cases. Since Fe(III) certainly binds Cl^- much more than Fe(II),[8b] the association constant of Cl^- is likely to be actually much smaller. This is the reason why reaction 1 was not investigated in NMA.

The determination of the two rate constants k_A and k_D was carried out either from the Fe^{II}/Fe^{I-} cathodic wave or from the $Fe^{II}Cl^-/Fe^{III}Cl$ anodic wave. In the first case, the complexation of Fe(II) with chloride ions has to be strong enough for the reduction of Fe(II) to show a kinetic character. Conversely, in the second case the complexation of Fe(II) by Cl^- has to be weak enough for the oxidation of $Fe^{II}Cl^-$ to show a kinetic character.

F. The first approach was used in a majority of cases. In the case where the kinetic character of the Fe^{II}/Fe^{I-} reduction wave appeared for Cl^- concentrations that are above 10 times that of the porphyrin, the theory developed for first-order CE mechanisms[12b,13b] was applied (procedure F1). In the case where the kinetic character of the Fe^{II}/Fe^{I-} wave appears without addition of Cl^- over the stoichiometric concentration, the theory for second-order conditions[13a] was applied (procedure F2).

Similar procedures were followed to treat the $Fe^{II}Cl^-/Fe^{III}Cl$ anodic wave, procedure F3 for first-order conditions and procedure F4 for second-order conditions. It has been previously shown that application of the two procedures to the same reaction gives concordant results.[11b]

All four procedures require that a large splitting of the wave into two waves be observed since the derivation of k_A and k_D is based on the measurement of the height of the kinetic wave. Overlapping of the two waves would then lead to large errors in k_A and k_D. This is what happens in the case of the a-$(C12)_2$-AC and a-$(C12)_2$-AT porphyrins in DMF (Figure 6). We then resorted to another method (procedure F5) based on the shift of the anodic peak featuring the oxidation of Fe(I) into Fe(II) upon addition of chloride ions to the solution. Figure 6d shows a typical example of the linear shift of the anodic peak potential with log $[Cl^-]$. It features an "EC" mechanism where the electron transfer (2) is followed by a chemical step (1), which is irreversible from left to right (Scheme I) under the present conditions. The peak potential, E_p, is then expressed as[17]

$$E_p = E°_{Fe^{II}/Fe^{I-}} + 0.78\frac{RT}{F} - \frac{RT}{2F}\ln\left(\frac{k_A[Cl^-]}{v}\frac{RT}{F}\right)$$

Since $E°_{Fe^{II}/Fe^{I-}}$ was previously determined according to procedure F2, the variations of E_p with $[Cl^-]$ (Figure 6c) immediately provide the value of k_A. k_D is then obtained from the previously determined value of K_A. It was checked on the example of a-$(C12)_2$-CT in DMF, where procedures F1 and F5 could be both applied, that they give the same result.

G. *The determination of the standard potential of the $Fe^{III}Cl/Fe^{III}Cl^-$ couple* was carried out from the anodic wave

(17) (a) Savéant, J. M.; Vianello, E. *C. R. Hebd. Seances Acad. Sci.* **1963**, *256*, 2597. (b) Nadjo, L.; Savéant, J. M. *J. Electroanal. Chem. Interfacial Electrochem.* **1973**, *48*, 113.

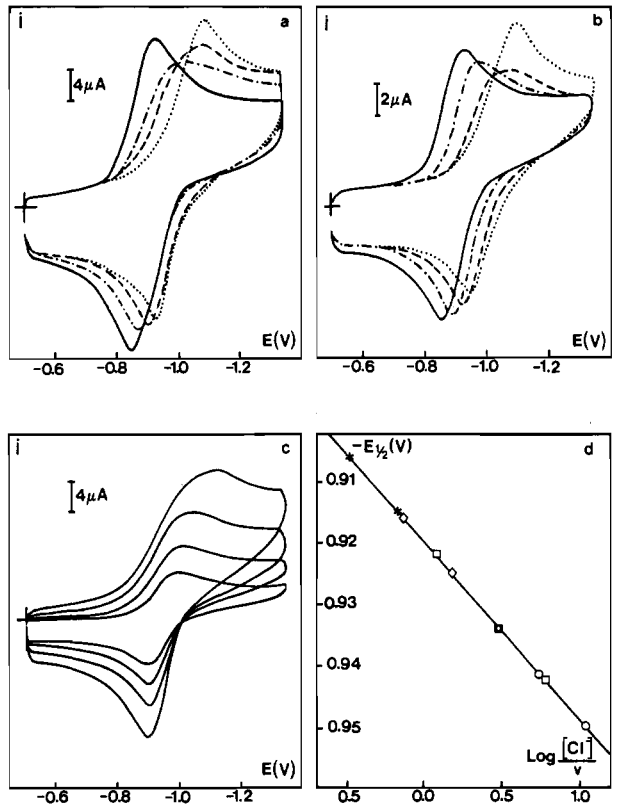

Figure 6. Cyclic voltammetry of the Fe^{II}/Fe^{I-} wave of the a-$(C12)_2$-AC and a-$(C12)_2$-AT basket-handle porphyrins in DMF (+0.1 M $LiClO_4$) at 20 °C: (a) AC (1 mM), without addition of Cl^- (—) and with 6 (-·-), 45 (- - -), and 300 (···) mM LiCl (sweep rate 0.4 $V.s^{-1}$); (b) AT (1 mM), without addition of Cl^- (—) and with 10 (-·-) 50 (- - -), and 500 (···) mM LiCl (sweep rate 0.1 $V.s^{-1}$); (c) AC (1 mM) variation with sweep rate in the presence of 30 mM LiCl (from bottom to top), v = 0.04, 0.1, 0.2, and 0.4 $V.s^{-1}$; (d) AC (1 mM) variations of the Fe^{I-}/Fe^{II} anodic peak potential with sweep rate and Cl^- concentration: (*) v = 0.1 and 0.2 $V.s^{-1}$, $[Cl^-]$ = 65 mM; (◇) v = 0.1, 0.2 , and 0.4 $V.s^{-1}$, $[Cl^-]$ = 0.3 M; (□) v = 0.1, 0.2, and 0.5 $V.s^{-1}$, $[Cl^-]$ = 0.6 M; (○) v = 0.1 and 0.2 $V.s^{-1}$, $[Cl^-]$ = 1.1 M.

featuring the oxidation of $Fe^{II}Cl^-$. When K_A is large, the wave is reversible and its half-wave potential is equal to the $E°$ without addition of Cl^- or with addition of a small amount of Cl^- (the latter then does not modify the half-wave potential). The procedure used under these conditions (procedure G1) simply consists in taking the midpoint between the anodic and cathodic peaks as a measure of $E°$. For smaller values of K_A but however sufficiently large for the wave to remain reversible $E°$ was derived from $E_{1/2}$ in the presence of excess Cl^- (procedure G2) from

$$E_{1/2} = E° - \frac{RT}{F} \ln \frac{K_A[Cl^-]}{1 + K_A[Cl^-]}$$

by using the value of K_A determined independently. For still smaller values of K_A, the wave splits into two waves, with the first having a kinetic character. $E°$ was then derived from the already described treatment of the kinetic wave. Procedure G3 then corresponds to the case where Cl^- is in excess, and procedure G4 to the case where it is not.

Discussion

We first discuss the thermodynamic features of reactions 1–4, namely the equilibrium constant of reaction 1 and the standard potentials of reactions 2–4 as a function of the structure of the porphyrin and of the solvent. The variations of the rate constants of reaction 1 with the structure of the porphyrins will be discussed further on.

The thermodynamic data pertaining to reactions 1–4 are listed in Table I so as to compare the ether-linked basket-handle porphyrins with TAP on one hand and the amide-linked superstructured porphyrins with TPP on the other. Free energy differences (numbers within parenthesis in Table I) are thus obtained, featuring the specific effect of the chains on each reaction, after elimination of the inductive effect of the substitution at the ortho position of the phenyl rings.[18]

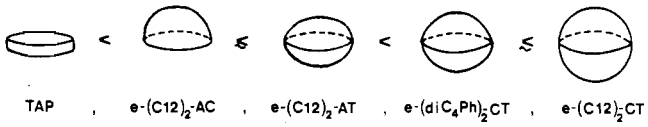

Figure 7. Schematic representation of the protection against solvation offered by the chains in basket-handle porphyrins.

It immediately appears that in all solvents all four reactions are made more difficult by the presence of the ether-linked chains, whereas they are oppositely favored by the presence of the amide-linked chains. The four reactions have in common that they involve an increase of the negative charge of the porphyrin complex when going from the left-hand to the right-hand side: from 0 to −1 with reactions 1, 2, and 4 and from −1 to −2 with reaction 3. The observed variations are thus explained by the variations in the solvation free energies of the porphyrin complexes: −1-charged complexes are more strongly solvated than the neutral complexes and less solvated than the −2-charged complexes. The ether-linked chains thus offer steric protection against the approach of the solvent molecules, thus decreasing the solvation free energy. The negatively charged species are thus destabilized, the doubly charged species more than the singly charged species, which renders all four reactions more difficult. With amide-linked structures a similar steric protection against solvation also exists. However, it is overcompensated by dipole–charge interactions involving the CONH groups and the negatively charged complexes, resulting in an overall stabilization of the latter species.

The results and rationalization first gained in an investigation where the solvent was DMF[8a] are thus confirmed by the present study, which demonstrates a similar behavior in four additional solvents. Closer inspection of the data shows that the degree of destabilization (ether-linked chains) or stabilization (amide-linked structures) of the negatively charged complexes is a function of both the porphyrin structure and the nature of the solvent. Their detailed analysis should thus lead to a better understanding of the mechanism of the protection offered by the chains against external solvation and of the "local solvation" brought about by the presence of the CONH groups.

Reaction 3, $Fe^{I-} + e^- \rightleftarrows Fe^{"0"\,2-}$, is the simplest case to be discussed since, axial coordination being absent in both the Fe^{I-} and $Fe^{"0"\,2-}$ complexes, the solvent simply acts as a solvating agent of the anionic species without interfering in their energetics as an axial ligand.

In the *ether-linked series*, the protection against solvation, as measured by $E°_{e\text{-}BHP} - E°_{TAP}$ (Table I), varies in DMF and PrCN, in the order e-$(C12)_2$-AC ≲ e-$(C12)_2$-AT < e-$(diC_4Ph)_2$-CT ≲ e-$(C12)_2$-CT.

In NMA, the order is the same with the exception of an inversion between e-$(C12)_2$-CT and e-$(diC_4Ph)_2$-CT. However, the most striking feature in this solvent is that the free energies of protection are smaller than those in the other solvents, particularly with the AC and AT structures.

The order found in DMF and PrCN suggests that the degree of protection increases as the volume statistically occupied by the chains increases, taking their possible random movements into account. Molecular models indeed indicate the order shown in

(18) (a) The Hammet σ coefficient of the NHCO substituent is practically zero.[18c] (b) The electron-donating inductive effect of the ether groups of the chains is expected to be actually somewhat smaller than that of the methoxy groups for two reasons: (i) they are less electron rich; (ii) the presence of the chains tends to hinder the rotation of the phenyl rings, thus decreasing the possibility of conjugation with the porphyrin ring. This difference is however expected to be small. It will, at worst, lead to a slight underestimation of the effect of the chains. The specific effect of the chains can thus be unambiguously distinguished from the possible difference in inductive effects. (c) Zuman, P. *Substituent Effects in Organic Polarography*; Plenum: New York, 1967; p 46.

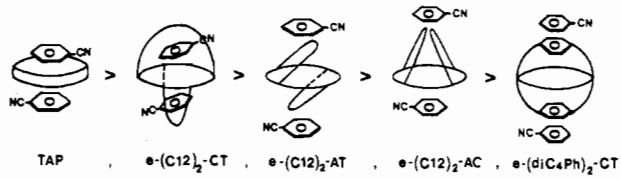

Figure 8. Schematic representation of the π–π^* interactions between benzonitrile and the $Fe^{0\,2-}$ TAP and basket-handle porphyrins.

Figure 7, which matches the order of the free energies of protection.

This first picture, where the chains exert a protecting effect not depending upon the solvent, is not in fact quite satisfactory, as shown by the results obtained with NMA. The anion-solvating ability of NMA appears to be much larger than that of DMF, PhCN, and PrCN.[19] One would thus expect, if the chains would offer constant protection, that the corresponding free energies be larger with NMA than with the other three solvents.[20] In fact, the opposite is observed, particularly in the case of the basket-handle porphyrins bearing the most flexible chains, i.e., e-$(C12)_2$-AC and e-$(C12)_2$-AT. We thus come to the concept that the protection offered by the chains is a function of the solvating power of the solvent and of the rigidity of the chains: the more "aggressive" the solvent in this respect and the more flexible the chains, the less efficient the protection. In other words, NMA is, to a larger extent than DMF and PrCN, able to thrust the chains aside or to flatten them out over the porphyrin ring, which is obviously easier with flexible than with rigid chains. The fact that the diC_4Ph chains offer more protection than the C12 chains anchored in the same positions in NMA and not in DMF and PrCN further confirms this picture.

In PhCN, the protection against solvation is strong but varies in a different order: e-$(C12)_2$-CT < e-$(C12)_2$-AT < e-$(C12)_2$-AC < e-$(diC_4Ph)_2$-CT. In contrast with the other solvents, we have now to take into account that benzonitrile is an aromatic molecule with a lack of electron density and an excess of positive charge in the π orbital owing to the electron-withdrawing character of the CN group. On the other hand, the Fe^{I-} and $Fe^{0\,2-}$ complexes possess an excess of electron density and negative charge in their π^* orbital, more in the second case than in first.[21] It is thus likely that solvation of the negatively charged porphyrins with benzonitrile involves, at least partially, π^*–π interactions with the two aromatic rings being parallel one to the other. These are expected to be much stronger in the case of $Fe^{0\,2-}$ than in that of Fe^{I-}. The order of protection free energies found in benzonitrile can thus be rationalized on these grounds, as shown schematically in Figure 8.

It is interesting to note, in this connection, how the standard potential of reaction 3 varies when passing from TPP to TAP, i.e., reacts to increase electron density in the porphyrin ring brought about by the four electron-donor methoxy groups in the ortho positions of the phenyl rings.[22]

solvent	DMF	NMA	PhCN	PrCN
$E^\circ_{TPP} - E^\circ_{TAP}$, mV	117	125	44	123

In all solvents, the potential difference is positive, indicating that the destabilization of $Fe^{0\,2-}$ by the introduction of electron-donor groups is larger than that of Fe^{I-}, which is anticipated from the electron density in the π^* porphyrin orbital being larger in the first complex than in the second. In all solvents, with the exception of PhCN, the potential difference is practically the same. This points to the conclusion that there is no specific interaction between the solvent molecules and the π^* orbital of the porphyrin that results in the solvation of the TPP and TAP and $Fe^{0\,2-}$ and Fe^{I-} complexes being practically the same. It is not the case with PhCN, for which the potential difference is significantly smaller than in the other solvents. This is compatible with the π^*–π interactions between the negatively charged porphyrin ring and the phenyl group in PhCN as invoked previously: owing to the increase of the electron density in the π^* orbital, the interaction would be enhanced when passing from TPP to TAP (more for $Fe^{0\,2-}$ than for Fe^{I-}), which should contribute to lower the intrinsic increase of the free energy.

The protection against solvation thus appears to be a function of the volume occupied by the chains, of their flexibility, and of the strength and mode of the interactions between the solvent molecules and the negatively charged porphyrins.

In the *amide-linked series*, the chains also protect the negatively charged complexes against solvation, but the ensuing destabilization is largely overcompensated by the stabilization that results from the dipole–charge interactions with the four secondary amide groups located in the close vicinity of the porphyrins ring. The fact that this local solvent effect is so strong is not very surprising in view of the strong ability of NMA to solvate negatively charged porphyrins as discussed before.

A first approach for estimating the magnitude of this local solvent effect on reaction 3 is to view the protection offered by chains as being solely a function of their average volume, as we

Table II. Effect of Amide Groups (Local Solvent Effect) on the Reaction $Fe^{I-} + e^- \rightleftarrows Fe^{0\,2-}$

$$(E^\circ_{a\text{-}BHP} - E^\circ_{TPP}) - (E^\circ_{e\text{-}BHP} - E^\circ_{TAP}) \quad \text{(in mV)}$$

Porphyrin \ Solvent	DMF 20°C	NMA 35°C	PhCN 20°C	PrCN 20°C
$(C12)_2$-AC	270	125	363	266
$(C12)_2$-AT	240	150	274	199
$(C12)_2$-CT	300	227	251	320
$(diC4Ph)_2$-CT	316	287	404	336

(19) (a) The acceptor number of NMA is much larger than those of DMF, PhCN, and PrCN.[7b] (b) Another token of the exceptionally large anion-solvating power of NMA is provided by the comparison of the potential separation between the Fe^{II}/Fe^{I-} and $Fe^{I-}/Fe^{0\,2-}$ couples in the two unprotected porphyrins, TPP and TAP. In mV:

	DMF	NMA	PhCN	PrCN
TPP	666	450	661	680
TAP	709	550	627	789

The potential separation is significantly smaller with NMA than with the other solvents, pointing to the larger stabilization of the anions by NMA (stabilization is larger for doubly charged $Fe^{0\,2-}$ than twice the stabilization for singly charged Fe^{I-}, as expected from a Born-type interaction with the solvent). Strictly speaking, the Fe^{II}/Fe^{I-} standard potential is also a function of the strength of the axial ligation of Fe(II) by the solvent. However, the complexing power is about the same for NMA and DMF[7a] and still the potential separation is much smaller in the first case than in the second. (c) Still another indication of the stronger anion-solvating power of NMA is, as discussed further on, the fact that Fe(II) and even Fe(III) are very weakly ligated by Cl^- ions in this solvent.

(20) For practical reasons, the temperature was higher in the case of NMA (35 °C) than with the other solvents (20 °C). This might change the free energies of protection. The change is however expected to be small: on one hand the solvation free energy will decrease with temperature, but on the other, due to an increase of the random motions of the chains, the protection should increase, compensating the first effect. That is indeed what we found on the example of TAP and e-$(C12)_2$-AT in PrCN; the free energy of protection is 136 mV at 35 °C as compared to 135 mV at 20 °C.

(21) Although, in the Fe^{I-} complex, the unpaired electron is delocalized over the porphyrin π^* orbital and the d_{z^2} iron orbital, the latter form appears to give the major contribution to the resonance.[4] In the case of the $Fe^{0\,2-}$ complex, the dominant resonant form appears to be the Fe(I) anion radical mesomeric structure.[4e,f,h,d]

(22) (a) Hammet relationships concerning the standard potentials of the various iron porphyrin redox couples have been previously investigated in the case of substituents in the para position of the phenyl rings.[22b] (b) Kadish, K. M. *Iron-Porphyrins*; Gray, H. B., Ed.; Addison-Wesley: Reading, PA, 1983; Part II, pp 211–219.

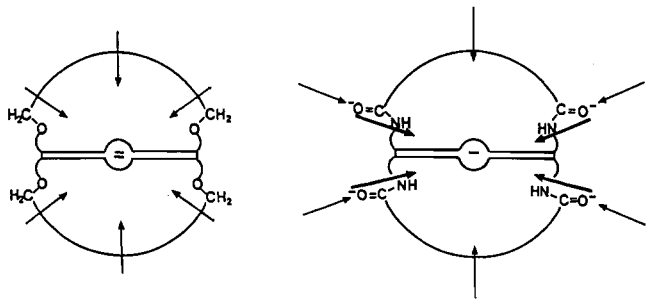

Figure 9. Steric protection against solvation, difference between ether-linked and amide-linked basket-handle porphyrins.

first did before. Under these conditions, the protection in the amide-linked series should be the same as in the ether-linked series for two compounds having the same number of carbons and the same arrangement of the chains. Thus

$$\Delta E^\circ = (E^\circ_{\text{a-BHP}} - E^\circ_{\text{TPP}}) - (E^\circ_{\text{e-BHP}} - E^\circ_{\text{TAP}})$$

would provide an estimate of the magnitude of the local solvent effect. This local solvation free energy, representing the specific interaction with the four amide groups, should thus be independent of the solvent and approximately[23] constant in the series of basket-handle porphyrins. It is seen (Table II) that although ΔE° remains of the same order of magnitude, significant differences appear when passing from one solvent to the other and from one basket-handle structure to the other.

Again, the data obtained in NMA are of particular interest. For all porphyrins, the ΔE°'s are smaller in NMA than in any of the other solvents. The difference is the most significant for the most flexible porphyrins, $(C12)_2$-AC and $(C12)_2$-AT. This indicates not only that NMA, owing to its particularly strong anion-solvating power, is able to overcome the steric barriers of the chains (especially when these are flexible) in the ether-linked series much more than other solvents, but also that this effect is significantly weaker in the amide-linked series than in the ether-linked series. This can be explained as illustrated schematically in Figure 9: since in the amide series the negative charge on the porphyrin is already interacting with the four CONH groups, there is less driving force for the solvent to overcome the steric barrier of the chains than in the ether series, where there is no local solvation. Also, owing to the polarizability of the CONH dipoles, a portion of the negative charge is transferred from the porphyrin ring to the periphery of the chains, at the level of the oxygen atoms of the amide groups.[24] As expected along these lines, the largest value of ΔE° is obtained with the $(diC_4Ph)_2$-CT porphyrins which, owing to the rigidity and the increased surface area of the chains provided by the phenyl groups, offer the most resistant protection to the approach of NMA molecules.[25]

The same trends appear, although less markedly, in DMF and in PrCN: the order in the ΔE°'s is the same as the order in protection found in the ether series, showing that also in these solvents the protection against solvation is larger in the amide series than in the ether-linked series for the same reason as in NMA. The effects are smaller because these two solvents are less "aggressive" as anion-solvating agents than NMA. This is also the reason why the $(C12)_2$-CT porphyrins offer more protection than the $(diC_4Ph)_2$-CT porphyrins in these two solvents whereas the opposite is true in NMA. In other words, rigidity of the chains is a less important factor in these two solvents than in NMA.

In PhCN also, the order of the ΔE°'s is the same as the order of protection against solvation found in the ether-linked series, showing that although the mode of solvation is somewhat different than with the other solvents, the protection is larger in the amide-linked series than in the ether-linked series, basically for the same reasons.

It follows that the maximal value of ΔE° can be taken as a minimal estimation of the free energy of the local solvent effect of the four amide groups on reaction 3. This is thus at least 0.4 eV, i.e., about 10^7 in terms of equilibrium constants at room temperature, showing that the local solvation effect of the amide groups is quite dramatic.[26]

It appears (Table I) that the standard potential of *reaction 2*, $Fe^{II} + e^- \rightleftarrows Fe^{I-}$, is likewise that of reaction 3, shifted negatively, by reference to TAP, by the presence of ether-linked chains and positively, by reference to TPP, by the presence of amide-linked chains. This suggests that the same protection and local solvation effects control reaction 2 at the level of the negatively charged Fe(I) complexes. The detailed interpretation of the variations of these effects with the solvent and the structure of the basket handles is however now complicated by an additional factor, viz., the axial ligation of iron(II) by a solvent molecule. The strength of this metal–ligand bond first depends upon the solvent. Moreover, it is likely to be also affected by the presence and structure of the basket handles if only for steric reasons, viz., the steric interaction between the chain and the axial ligand.

DCE being an extremely poor Lewis base,[7a] this problem does not arise in this solvent. Quite large protection effects are observed in the *ether-linked series* (Table I) related to the good ability of DCE to solvate anions.[7b] As expected from the above discussion of reaction 3, the e-$(C12)_2$-CT isomer offers better protection than the e-$(C12)_2$-AC isomer.

The effect of increasingly strong complexation of iron(II) by the coordinating solvent molecule is to shift the Fe^{II}/Fe^{I-} wave toward negative potentials. In the ether-linked series, steric hindrance to axial ligation by the solvent should thus shift the Fe^{II}/Fe^{I-} couple positively by reference to the unencombered TAP, i.e., compensating, at least partially, the negative shift due to the protection against solvation of the negatively charged Fe(I) complex. The magnitude of the potential shift caused by steric hindrance to axial coordination is expected to be a function both of the structure of the chains and of the coordinating ability of the solvent. This is likely to follow the order PrCN < PhCN < NMA $\lesssim$ DMF, as results both from the spectroscopic results described in the preceding section and from the rough estimate provided by the donor numbers.[7a]

There is clear evidence that steric hindrance to axial ligation does play a role in the influence of the chains on reaction 2. For all porphyrins, the values of $\Delta E^\circ = E_{\text{e-BHP}} - E_{\text{TAP}}$ (Table I) are less negative for DMF than PhCN and for PhCN than PrCN; i.e., the order is the same as the coordinating ability of these three solvents, for which the protection effects should not be very different since their acceptor numbers are about the same.[7b]

The small (absolute) values of ΔE° observed in the case of NMA (Table I) are a consequence both of its good coordinating power (similar to that of DMF) and of the fact that protection against solvation is not very efficient, especially for the most flexible structures, owing to the strong anion-solvating ability of this solvent. The latter effect is the same as already discussed for reaction 3, although it should act less dramatically in the present case since interaction is now with a single negative charge

(23) The CONH groups are not exactly arranged in the same manner in all the investigated amide-linked basket-handle porphyrins, two on each side of the porphyrin ring in the AT and CT configurations, four on one side in the AC and the PF configuration. Moreover, the average direction of the CONH dipole may not be exactly the same in the $(C12)_2$-AT, $(C12)_2$-CT, and $(diC_4Ph)_2$-CT porphyrins.

(24) Interaction between these negative charges and external solvent molecules could modulate the strength of the interaction between the CONH dipoles and the porphyrin charge as a function of the solvent. This effect is however expected to be small since polarization of the CONH dipole by the porphyrin negative charge is likely to be much more effective than polarization by the external solvent dipoles.

(25) This is further confirmed by an experiment carried out in NMA with two additional porphyrins bearing, in a CT configuration, one C12 chain on one side and a diC_3py chain (py = pyridine attached to the carbon chains at the 3 and 3′ positions) on the other. From the $E^\circ_{Fe^{I-}/Fe^{0}}$ values obtained with the ether-linked and amide-linked versions of these basket-handles, ΔE° results to be 257 mV, i.e., as expected, just between the values obtained with $(C12)_2$-CT and $(diC_4Ph)_2$-CT (Table II).

(26) Larger than previously estimated ($\simeq$0.3 eV) from experiments in DMF in the analysis of which the difference in protection between the ether-linked and amide-linked basket-handle porphyrins was not taken into account.[8a]

Table III. Effect of the Chains Caused by Steric Hindrance to Axial Ligation by Solvent on the Reaction $Fe^{II} + e^- \rightleftarrows Fe^{I-}$

$$\Delta E^\circ = (E^\circ_{a\text{-}BHP} - E^\circ_{TPP}) - (E^\circ_{e\text{-}BHP} - E^\circ_{TAP}) \text{ in mV}$$

Solvent / Porphyrin	DMF	NMA	PhCN	PrCN	DCE
$(C12)_2$-AC	178	140	286	298	312
$(C12)_2$-AT	166	155	291	293	—
$(C12)_2$-CT	165	190	266	294	358
$(diC4Ph)_2$-CT	113	155	188	274	—

instead of two in the previous case.

Another piece of evidence of the role of steric hindrance to axial coordination is the particularly small values of $|\Delta E^\circ|$ observed with the e-$(diC_4Ph)_2$-CT porphyrin (Table I). Moreover, these values decrease as the coordinating power of the solvent increases. The case of NMA is particularly striking: whereas the e-$(diC_4Ph)_2$-CT basket handle was shown to offer the best protection against solvation by NMA (maximal value of $|\Delta E^\circ|$ for reaction 3), the smallest value of $|\Delta E^\circ|$ is now obtained with this very porphyrin. This particular behavior of the e-$(diC_4Ph)_2$-CT structure emphasizes the role of steric hindrance to axial coordination since this is expected to reach its maximum in the series for this particular structure owing to the rotation of the phenyl rings in the basket-handle chains.

The case of the AC isomer is worth particular comment. Since it is protected on only one face, $|\Delta E^\circ|$ should not vary significantly if the unprotected porphyrins were ligated by a single solvent molecule. It is observed that $|\Delta E^\circ|$ actually decreases when passing from DCE and PrCN to PhCN and DMF. This points to the possibility that two solvent molecules may coordinate Fe(II). As discussed in ref 8a and in the references cited therein, investigation of the coordination of Fe(II) porphyrins by DMF in noncoordinating solvents indicates ligation by a single DMF molecule. It is not however excluded that in the pure solvent a second molecule may also coordinate the iron(II).

In the *amide-linked series*, steric hindrance to axial coordination should also interfere besides the protection and local solvent effects. A first attempt to estimate the magnitude of these factors is to examine the variations of the free energy

$$\Delta E^\circ = (E^\circ_{a\text{-}BHP} - E^\circ_{TPP}) - (E^\circ_{e\text{-}BHP} - E^\circ_{TAP})$$

with the solvent and the basket-handle structure (Table III). If the protection against external solvation and the steric hindrance to axial coordination were the same in the ether-linked and amide-linked series, ΔE° should remain constant. It is seen that its variations are not very large, showing that the protection and the steric hindrance to axial ligation do not change considerably when passing from one series to the other. The protection against solvation is indeed expected to change less than in case of reaction 3 where a double-charged species is involved. The observed variations are however well beyond the experimental uncertainty and are worth some comments.

It is noticed that the ΔE°'s are significantly smaller in the strongly coordinating solvent DMF not only than in the noncoordinating solvent DCE but also than in the less coordinating solvents PrCN and PhCN, which have acceptor numbers comparable to that of DMF.[7b] On the other hand, the values obtained with the $(diC_4Ph)_2$-CT structure are remarkably small as compared to those obtained with the $(C12)_2$-CT structure in view of the fact that the total of the local solvent effect and of the difference in protection between the amide-linked and corresponding ether-linked chains should be about the same in both cases.

This suggests that the effect of steric hindrance to axial ligation is stronger in the case of the ether-linked basket-handle cases than in the case of the corresponding amide-linked structures. Since

Table IV. Steric Hindrance of $Fe^{II}Cl^-$ Coordination by diC_4Ph Chains

Solvent	DMF	PhCN	PrCN
$\frac{RT}{F} \ln\left(\frac{K_A^{e\text{-}(C12)_2\text{-}CT}}{K_A^{e\text{-}(diC4Ph)_2\text{-}CT}}\right)$ a	48	41	40
$\frac{RT}{F} \ln\left(\frac{K_A^{a\text{-}(C12)_2\text{-}CT}}{K_A^{a\text{-}(diC4Ph)_2\text{-}CT}}\right)$ a	60	140	95

a : in mV

the flexibility of the chains is either the same in the two series or slightly smaller in the amide case, we are led to conclude that the presence of the amide dipoles tends to strengthen the axial coordinate of iron(II) with neutral ligands.[27]

Taking the above remarks into account, inspection of Table III allows one to conclude that the minimal value of the effect of the CONH group on the $Fe^{II} + e^- \rightleftarrows Fe^{I-}$ reaction is about 360 mV (10^6 in terms of equilibrium constant).

Reaction 1, $Fe^{II} + Cl^- \rightleftarrows Fe^{II}Cl^-$, as reactions 2 and 3, is rendered more difficult, with reference to TAP, by the presence of ether-linked chains and easier, with reference to TPP, by the presence of amide-linked chains. The dominant effects controlling the reactivity are thus, here again, the protection against external solvation and the local solvent effect of the amide groups, on the basis of the fact that the charge of the porphyrin passes from 0 to −1 during reaction 1. It is however expected that steric hindrance to axial ligation at iron(II) be an additional controlling factor, steric hindrance to axial coordination by solvent molecules as with reaction 2 but also steric hindrance to axial coordination of Fe(II) by chloride ions.

The addition and possible mutual influence of all these effects preclude a detailed analysis of the variations of the free energy featuring the specific effect of the chains, $(RT/F) \ln (K_A^{e\text{-}BHP}/K_A^{TAP})$ and $(RT/F) \ln (K_A^{a\text{-}BHP}/K_A^{TPP})$, as a function of the solvent and of the nature and configuration of the chains (Table I), as done for reactions 1 and 2. However, the steric hindrance to coordination of Cl^- with Fe(II) is clearly visible upon comparison between the $(C12)_2$-CT and $(diC_4Ph)_2$-CT structures in the ether-linked and amide-linked series (Table IV). The two structures have similar capabilities concerning both protection against external solvation and local solvation by the CONH groups. They differ very significantly regarding steric hindrance of the coordination of the iron atom with axial ligand, expecially for small ligands such as Cl^-. It is seen from molecular models that steric hindrance to Cl^- coordination is weak with the $(C12)_2$-CT structure and strong with the $(diC_4Ph)_2$-CT structure, owing to the rotation of the phenyl ring of the chains in the latter case. With bulkier ligands such as the solvent molecules the difference between the steric hindrance by the two types of chains is much smaller. In other words, the $(C12)_2$-CT chains exert a steric discrimination between the solvent molecules and Cl^- ions as axial ligand, whereas the $(diC_4Ph)_2$-CT chains do it to a much lesser extent. These are the reasons why association with Cl^- ions is weaker with $(diC_4Ph)_2$-CT structures than with $(C12)_2$-CT structures in both the ether-linked and amide-linked series (Table IV). That the effect is larger in the latter than in the former case simply results from the fact that coordination with Cl^- is stronger: the presence of the amide-linked chains stabilizes the $Fe^{II}Cl^-$ complex whereas the ether-linked chains have the opposite effects, as observed and rationalized above.

(27) (a) This is confirmed by recent experiments indicating that axial coordination of iron(II) by the neutral ligand 1,2-dimethylimidazole is enhanced by the presence of a basket handle bearing secondary amide groups.[27b] (b) Lexa, D.; Momenteau, M.; Savéant, J. M.; Xu, F. *J. Am. Chem. Soc.*, in press.

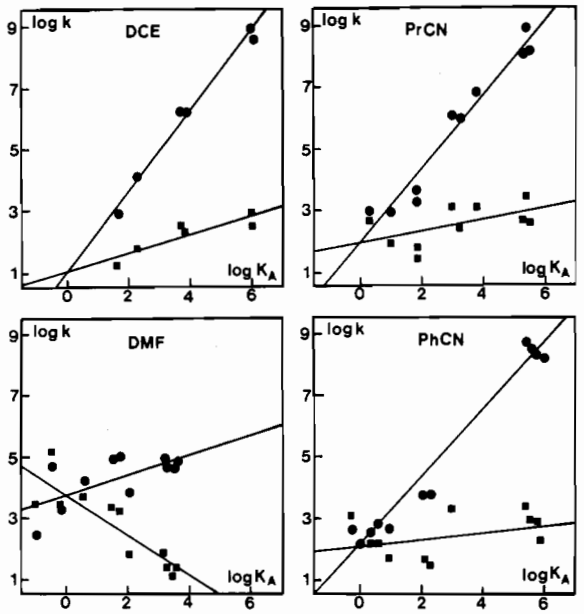

Figure 10. Plots of log k_A (●) and log k_D (■) vs. log K_A for the reaction (S)Fe^{II} + Cl^- ⇄ $Fe^{II}Cl^-$ + (S) in the four solvents DCE, PrCN, PhCN, and DMF.

The *effect of the chains on the* $Fe^{III}Cl + e^- \rightleftarrows Fe^{II}Cl^-$ *reaction* is another example of protection against solvation and "local solvation". The standard potential is indeed systematically shifted negatively, as compared to TAP, in the ether-linked series and positively, as compared to TPP, in the amide-linked series. As expected, the nature of the solvent does not exert a strong influence on the observed shifts in both series. Their values are likely, besides the above solvation effect, to be a function of the steric hindrance exerted by the chains toward coordination of Cl^- with Fe(III) and Fe(II) and possibly by solvent molecules in the sixth position.

The *effect of the chains on the kinetics of reaction 1*

$$(S)Fe^{II} + Cl^- \underset{k_D}{\overset{k_A}{\rightleftharpoons}} Fe^{II}Cl^- + (S)$$

(S = coordinating solvent molecule) is expected to involve the same type of factors, protection against external solvation, "local solvation", and steric hindrance to axial coordination, that have been shown to control the equilibrium constant. For this very reason, the large number of possibly interacting factors that are involved again precludes a detailed analysis of the effects of the superstructures. However, some interesting trends appear upon inspection of the kinetic data. These are best seen by representing the results under the form of activation vs. driving force free energy relationships, i.e., as log k_A and log k_D vs. log K_A plots. These are shown in Figure 10 for each of the four solvents. log k_A and log k_D exhibit a rough linear correlation with log K_A, confirming the involvement of the same three factors (protection against external solvation, "local solvation" by the CONH groups, steric hindrance to axial coordination) in the kinetics as in the thermodynamics of the reaction.

A comparison of the correlation in DCE, a noncoordinating solvent, and in DMF, a good coordinating solvent (Figure 10), shows two significantly different behaviors.

In DCE, an increase of K_A results in a large increase of k_A and a small increase in k_D. This is what is expected for a reaction where Cl^- reacts with a four-coordinated Fe(II) complex (Figure 11a), and thus the transition state resembles the final state from the point of view of solvation, which is then the main variable factor in the series. In this context, the fact that log k_A varies

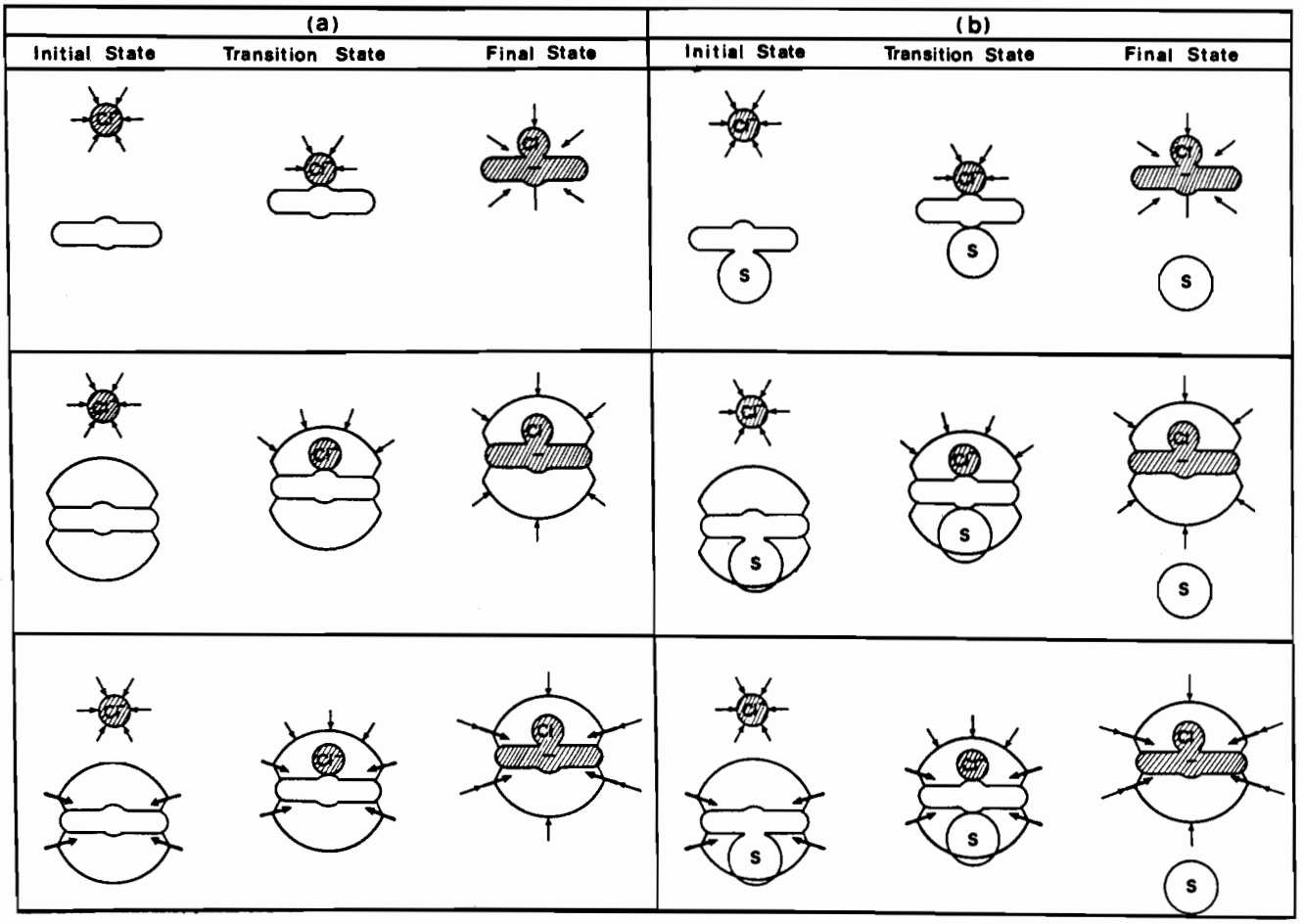

Figure 11. Schematic representation of the initial state, transition state, and final state for the unprotected, ether-linked, and amide-linked superstructured porphyrins for the reaction (S)Fe^{II} + Cl^- ⇄ $Fe^{II}Cl^-$ + (S): (a) reaction of Cl^- with a four-coordinated Fe(II) porphyrin (noncoordinating solvent); (b) S_N2 displacement of a solvent molecule (S) by Cl^-.

more rapidly than log K_A (correlation slope ~1.3) and log k_D increases with log K_A (correlation slope ~0.3) is explained by the larger concentration of the negative charge in the transition state than in the final state. In the former, the negative charge is located in the Cl^- ion, whereas in the latter, part of it is delocalized over the iron atom and the porphyrin ring. It follows that protection against external solvation as well as "local solvation" by the CONH groups is larger in the transition state than in the final state (Figure 11a). Thus, in the ether-linked series, the increase of the activation free energy due to protection against solvation is larger than the corresponding decrease of the driving force. Vice-versa, in the amide-linked series the decrease of the activation free energy due to interaction of the negative charge with the CONH dipoles is larger than the corresponding decrease of the driving force.

In DMF, log k_A increases much less markedly with log K_A (correlation slope ~0.3) whereas log k_D now decreases with log K_A (correlation slope ~−0.7). This is compatible with a S_N2-type process where Cl^- replaces a DMF molecule in a five-coordinated complex (Figure 11b) since the transition state then still resembles the final state from the point of view of solvation but resembles the initial state from the point of view of axial coordination with a solvent molecule (Figure 11b).

The behavior observed in PrCN (Figure 10) is very similar to that in DCE, the correlation slopes being slightly smaller (1.2 and 0.2 for k_A and k_D, respectively). This is again compatible with an S_N2 process in which, however, the role of axial ligation by the solvent molecule as compared to that of solvation would be much weaker than in DMF, paralleling the complexing powers of the two solvents. In PhCN, too, the variations of k_A and k_D with K_A are of the same type, the correlation slopes being somewhat smaller than in PrCN (1.1 and 0.1 for k_A and k_D, respectively), which falls in line with the complexing power of PhCN being stronger than that of PrCN and smaller than that of DMF.

Conclusions

The main conclusions of this study are as follows.

(i) The thermodynamics of the four investigated reactions, $Fe^{III}Cl + e^- \rightleftarrows Fe^{II}Cl^-$, $Fe^{II} + Cl^- \rightleftarrows Fe^{II}Cl^-$, $Fe^{II} + e^- \rightleftarrows Fe^{I-}$, and $Fe^{I-} + e^- \rightleftarrows Fe^{*0*\,2-}$, are strongly affected, in all investigated solvents, by the presence of the basket-handle structures attached to the porphyrin ring.

(ii) For all four reactions, which correspond to the creation of a negative charge in the porphyrin complex, the change in reactivity is mainly governed by the changes in solvation of the anionic species brought about by the presence of the basket-handle superstructure. In the ether-linked series, the effect of the chains, in this connection, is to sterically protect the anionic porphyrins against solvation, which rendered all four reactions more difficult than those with the unprotected porphyrins. The same effect appears in the amide-linked series but is largely overcompensated by the interaction of the negative charges with the secondary amide dipoles, resulting in a local solvation that makes all four reactions easier than those with the bare porphyrins.

(iii) These external and local solvation factors exlusively control the effect of the chains on the reactivity of the Fe^{I-} and $Fe^{*0*\,2-}$ complexes, as revealed by the investigation of the $Fe^{I-} + e^- \rightleftarrows Fe^{*0*\,2-}$ reaction. It then appeared, upon observation of the variation of the reactivity with the structure and spatial arrangement of the basket-handle chains, that the protection against solvation is primarily governed by the average volume they occupy. This is not however the only factor. Protection against solvation also depends jointly upon the nature of the solvent and the flexibility of the chains: the more solvating the solvent and the more flexible the chains, the lower the protection. Another important observation is that the amide-linked structures offer better protection than the corresponding ether-linked structures owing to the fact that local solvation by the CONH groups weakens the propensity of the external solvent to interact with the negatively charged porphyrins. It can thus be estimated that a lower limit of the free energy of the local solvation effect of the four CONH group on the reaction is 0.4 eV, i.e., about 10^7 in terms of equilibrium constant at room temperature.

(iv) The thermodynamics of the $Fe^{II} + e^- \rightleftarrows Fe^{I-}$ and $Fe^{II} + Cl^- \rightleftarrows Fe^{II}Cl^-$ reactions are also mainly affected by the same external and local solvation factors. However, the effect of the chains on the reactivity is additionally a function of the steric hindrance they created against the axial coordination of the iron(II) porphyrins, steric hindrance to the axial coordination of solvent molecules and steric hindrance to the binding of Cl^-. It appears that a minimal value of the effect of the CONH dipoles on the $Fe^{II} + e^- \rightleftarrows Fe^{I-}$ reaction is 0.36 eV, i.e., about 10^6 in terms of equilibrium constant at room temperature. It can be estimated that the free energy of interaction of the four CONH groups with one negative charge is about 1.4 eV in vacuo, assuming that the CONH groups are rigidly oriented with the most favorable angle toward a negative charge located on the iron atom. This could be somewhat overestimated since the orientation may be less favorable and the charge located in another manner, not however so as to reach the experimental value of 0.36–0.4 eV found for the present reaction and the preceding one even though these figures can be somewhat underestimated, as discussed earlier. The observation that the experimental value is about 30% of the value predicted in vacuo underlines that although the solvent still interferes in the interaction between the CONH groups and the central charge, this interference is quite small, corresponding to an enormously reduced average dielectric constant.

(v) The effect of the basket-handle structures on the kinetics of the $Fe^{II} + Cl^- \rightleftarrows Fe^{II}Cl^-$ reaction involve essentially the same factors as those influencing its thermodynamics. In noncoordinating solvents, the transition state resembles the final state and is likewise influenced by protection against external solvation, local solvation, and steric hindrance to Cl^- coordination. In coordinating solvents, the transition state resembles the final state vis-ã-vis the same factors but resembles the initial state vis-ã-vis the steric hindrance against coordination by a solvent molecule.

It is remarkable that relatively simple superstructures such as the basket-handle chains investigated here strongly influence the reactivity of the central iron complex, exhibiting various of the functions that are expected to be those of the protein chains toward the prosthetic group in metalloproteins: protection vis-ã-vis the external environment, "local solvation" effects of the secondary amide groups, and steric control of axial coordination.

Experimental Section

Instrumentation, cells, electrodes for cyclic voltammetry, and thin-layer spectroelectrochemistry were the same as previously described.[8] All potentials are referred to the aqueous NaCl saturated calomel electrode.

The supporting electrolytes, $LiClO_4$ and NBu_4ClO_4, were from commerical origin. $LiClO_4$ was used as received, whereas NBu_4ClO_4 was recrystallized in ether–acetone before use and dried under vacuum at 40 °C.

The solvents were from commercial origin. DMF (Carlo Erba, reagent grade) was used as received. PhCN was refluxed on P_2O_5 for 3 days and distilled. PrCN and NMA were purified as described in ref 28a and b, respectively.

The synthesis and characterization of the porphyrins investigated in this work have already been described: TAP, TPP,[29a] e-BHP,[29b] a-BHP,[29c] a-PF.[29d]

Registry No. TAP-$Fe^{III}Cl$, 90837-94-8; TAP-Fe^{II}, 104423-64-5; TAP-Fe^{II}DMF, 90838-08-7; TAP-Fe^{II}NMA, 104423-61-2; TAP-Fe^{II}PhCN, 104423-62-3; TAP-Fe^{II}PrCN, 104423-63-4; $[TAP\text{-}Fe^{I}]^-$, 90838-00-9; $[TAP\text{-}Fe^{0}]^{2-}$, 90838-04-3; TPP-$Fe^{III}Cl$, 16456-81-8; TPP-Fe^{II}, 16591-56-3; TPP-Fe^{II}DMF, 90838-16-7; TPP-Fe^{II}NMA, 104423-68-9; TPP-Fe^{II}PhCN, 104423-74-7; TPP-Fe^{II}PrCN, 104423-83-8; $[TPP\text{-}Fe^{I}]^-$, 54547-68-1; $[TPP\text{-}Fe^{0}]^{2-}$, 90838-22-5; a-PF-$Fe^{III}Cl$, 104486-25-1; a-PF-Fe^{II}DMF, 104486-28-4; a-PF-Fe^{II}NMA, 104423-69-0; a-

(28) (a) Van Duyne, R.; Reilley, C. N. *Anal. Chem.* **1972**, *44*, 142. (b) Knecht, L. A.; Kolthoff, I. M. *Inorg. Chem.* **1962**, *1*, 195.

(29) (a) Adler, A. D.; Longo, F. R.; Finarelli, J. D.; Assour, J.; Korsakoff, L. *J. Org. Chem.* **1967**, *32*, 476. (b) Momenteau, M.; Mispelter, J.; Loock, B.; Bisagni, E. *J. Chem. Soc., Perkins Trans. 1* **1983**, 189. (c) Momenteau, M.; Mispelter, J.; Loock, B.; Lhoste, J. M. *J. Chem. Soc., Perkins Trans. 1* **1985**, 221. (d) Collman, J. P.; Gagnê, R. R.; Halper, T. R.; Marchon, J. C.; Reed, C. A. *J. Am. Chem. Soc.* **1973**, *95*, 7868.

PF-Fe^{II}PhCN, 104423-75-8; [a-PF-Fe^{I}]$^-$, 90857-60-6; [a-PF-Fe^{0}]$^{2-}$, 90838-25-8; e-$(C12)_2$-AC-Fe^{III}Cl, 104486-31-9; e-$(C12)_2$-AC-Fe^{II}, 104486-36-4; e-$(C12)_2$-AC-Fe^{II}DMF, 104486-27-3; e-$(C12)_2$-AC-Fe^{II}NMA, 104423-65-6; e-$(C12)_2$-AC-Fe^{II}PhCN, 104423-72-5; e-$(C12)_2$-AC-Fe^{II}PrCN, 104423-79-2; [e-$(C12)_2$-AC-Fe^{I}]$^-$, 90838-01-0; [e-$(C12)_2$-AC-Fe^{0}]$^{2-}$, 104486-30-8; e-$(C12)_2$-AT-Fe^{III}Cl, 104486-32-0; e-$(C12)_2$-AT-Fe^{II}DMF, 90898-40-1; e-$(C12)_2$-AT-Fe^{II}NMA, 104486-33-1; e-$(C12)_2$-AT-Fe^{II}PhCN, 104486-35-3; e-$(C12)_2$-AT-Fe^{II}PrCN, 104423-80-5; [e-$(C12)_2$-AT-Fe^{I}]$^-$, 104486-29-5; [e-$(C12)_2$-AT-Fe^{0}]$^{2-}$, 90898-39-8; e-$(C12)_2$-CT-Fe^{III}Cl, 79198-03-1; e-$(C12)_2$-CT-Fe^{II}, 70196-65-5; e-$(C12)_2$-CT-Fe^{II}DMF, 90838-10-1; e-$(C12)_2$-CT-Fe^{II}NMA, 104423-66-7; e-$(C12)_2$-CT-Fe^{II}PhCN, 104438-55-3; e-$(C12)_2$-CT-Fe^{II}PrCN, 104423-81-6; [e-$(C12)_2$-CT-Fe^{I}]$^-$, 79209-91-9; [e-$(C12)_2$-CT-Fe^{0}]$^{2-}$, 90838-06-5; e-$(diC_4Ph)_2$-CT-Fe^{III}Cl, 83460-51-9; e-$(diC_4Ph)_2$-CT-Fe^{III}OH, 104423-88-3; e-$(diC_4Ph)_2$-CT-Fe^{II}DMF, 90838-11-2; e-$(diC_4Ph)_2$-CT-Fe^{II}NMA, 104423-67-8; e-$(diC_4Ph)_2$-CT-Fe^{II}PhCN, 104423-73-6; e-$(diC_4Ph)_2$-CT-Fe^{II}PrCN, 104423-82-7; [e-$(diC_4Ph)_2$-CT-Fe^{I}]$^-$, 90838-03-2; [e-$(diC_4Ph)_2$-CT-Fe^{0}]$^{2-}$, 90838-07-6; a-$(C12)_2$-AC-Fe^{III}Cl, 104486-26-2; a-$(C12)_2$-AC-Fe^{II}, 104423-86-1; a-$(C12)_2$-AC-Fe^{II}DMF, 90898-43-4; a-$(C12)_2$-AC-Fe^{II}NMA, 104423-70-3; a-$(C12)_2$-AC-Fe^{II}PhCN, 104423-76-9; a-$(C12)_2$-AC-Fe^{II}PrCN, 104527-26-6; [a-$(C12)_2$-AC-Fe^{I}]$^-$, 90898-44-5; [a-$(C12)_2$-AC-Fe^{0}]$^{2-}$, 90898-45-6; a-$(C12)_2$-AT-Fe^{III}Cl, 90838-13-4; a-$(C12)_2$-AT-Fe^{II}DMF, 90838-18-9; a-$(C12)_2$-AT-Fe^{II}NMA, 104486-34-2; a-$(C12)_2$-AT-Fe^{II}PhCN, 104423-77-0; a-$(C12)_2$-AT-Fe^{II}PrCN, 104423-84-9; [a-$(C12)_2$-AT-Fe^{I}]$^-$, 104423-57-6; [a-$(C12)_2$-AT-Fe^{0}]$^{2-}$, 90838-24-7; a-$(C12)_2$-CT-Fe^{III}Cl, 90838-12-3; a-$(C12)_2$-CT-Fe^{II}, 93646-94-7; a-$(C12)_2$-CT-Fe^{II}DMF, 90838-17-8; a-$(C12)_2$-CT-Fe^{II}NMA, 104438-54-2; a-$(C12)_2$-CT-Fe^{II}PhCN, 104438-56-4; a-$(C12)_2$-CT-Fe^{II}PrCN, 104438-57-5; [a-$(C12)_2$-CT-Fe^{I}]$^-$, 90838-20-3; [a-$(C12)_2$-CT-Fe^{0}]$^{2-}$, 90838-23-6; a-$(diC_4Ph)_2$-CT-Fe^{II}Cl, 104423-60-1; a-$(diC_4Ph)_2$-CT-Fe^{III}OH, 104423-87-2; a-$(diC_4Ph)_2$-CT-Fe^{II}DMF, 104423-56-5; a-$(diC_4Ph)_2$-CT-Fe^{II}NMA, 104423-71-4; a-$(diC_4Ph)_2$-CT-Fe^{II}PhCN, 104423-78-1; a-$(diC_4Ph)_2$-CT-Fe^{II}PrCN, 104423-85-0; [a-$(diC_4Ph)_2$-CT-Fe^{I}]$^-$, 104423-58-7; [a-$(diC_4Ph)_2$-CT-Fe^{0}]$^{2-}$, 104423-59-8; Cl^-, 1112-67-0; NBu_4ClO_4, 1923-70-2; $LiClO_4$, 7791-03-9.

Notes

Contribution from the Departments of Chemistry, Stanford University, Stanford, California 94305, and University of South Carolina, Columbia, South Carolina 29208

Iron–Sulfur Bond Lengths in Ferrous–CO Heme Complexes as a Function of Sulfur Donor Type

Lung-Shan Kau,[1a] Edmund W. Svastits,[1b] John H. Dawson,*[1b] and Keith O. Hodgson*[1a]

Received March 20, 1986

The structural characterization of iron coordination is of considerable importance in understanding the mechanism of action of heme iron enzymes. To that end, metalloporphyrin complexes have been used extensively as both structural and functional models for heme proteins since their ligand composition can be more easily varied than that of the proteins they are intended to mimic.

The role of sulfur donor ligation in the function of heme proteins is incompletely understood at present. For example, both cytochrome P-450 (P-450)[2,3] and secondary amine monooxygenase[4] catalyze reduced pyridine nucleotide- and O_2-dependent N-dealkylation reactions but have different axial heme ligands (cysteinate and histidine, respectively). In contrast, the spectroscopic similarities between P-450 and chloroperoxidase have suggested an identical heme coordination structure for the two enzymes (pentacoordinate, cysteinate ligated),[5] despite their functional differences (monooxygenase and peroxidase, respectively).

To date, only a very small number of sulfur-donor-ligated ferrous porphyrins have been structurally defined. Weiss and co-workers[6,7] have used X-ray crystallography to investigate penta- and hexacoordinate ferrous porphyrin thiolate complexes, with CO and O_2 trans to thiolate in the latter case. For ferrous porphyrin complexes containing neutral sulfur donors, only the hexacoordinate bis(thioether),[8] thioether/imidazole,[8] and thioether/O_2[9] adducts have been structurally characterized. No such investigations of ferrous porphyrin complexes containing a dialkyl disulfide axial ligand have appeared; neither have the previously reported hexacoordinate thiol/CO[10,11] and thioether/CO[11] complexes been structurally defined. The present report substantially increases this database of Fe(II)–S bond distances to include ferrous porphyrin adducts having thiol, thioether, and disulfide ligands trans to CO. All three of these sulfur donor types represent potential axial ligands in biological systems. The Fe(II)–S bond length has been found to vary systematically as a function of the sulfur donor type.

The method we have employed for this structural analysis of sulfur-ligated heme complexes is extended X-ray absorption fine structure (EXAFS) spectroscopy, a technique that has been previously shown to accurately probe the iron coordination environment of heme proteins and metalloporphyrins.[12] The EXAFS spectra contain local structural information about the type, number, and distance of atoms surrounding the absorbing Fe atom. These spectra can be collected on solutions in a short time and provide accurate metrical details. In contrast, protein crystallographic studies require good single crystals and the diffraction data analysis and refinement are lengthy processes. A limitation of the EXAFS technique is its inability to discriminate between atoms adjacent in the periodic table (e.g. C, N, O) due to their similar backscattering properties; however, this is not a problem in sulfur-ligated heme complexes since the contributions of the axial sulfur (S_{ax}) and porphyrin pyrrole and axial ligand nitrogens

(1) (a) Stanford University. (b) University of South Carolina.
(2) Dawson, J. H.; Eble, K. S. *Adv. Inorg. Bioinorg. Mech.* **1986**, *4*, 1-64.
(3) Abbreviations: DMA, *N*,*N*-dimethylacetamide; EtS^-, ethanethiolate; EXAFS, extended X-ray absorption fine structure; L_{ax}, axial ligand; MeSSMe, dimethyl disulfide; *N*, the number of ligand atoms; N_{ax}, axial nitrogen donor; N_p, porphyrin pyrrole nitrogen; OEP, octaethylporphyrinato; P-450, cytochrome P-450; PrS^-, propanethiolate; PrSH, propanethiol; S_{ax}, axial sulfur donor; THT, tetrahydrothiophene; TpivPP, *meso*-tetrakis($\alpha,\alpha,\alpha,\alpha$-*o*-pivalamidophenyl)porphyrinato; TPP, *meso*-tetraphenylporphyrinato; TPP(C5Im), imidazole-tailed TPP; TTP, *meso*-tetra-*p*-tolylporphyrinato.
(4) (a) Brook, D. F.; Large, P. J. *Eur. J. Biochem.* **1975**, *55*, 601–609. (b) Alberta, J. A.; Andersson, L. A.; Dawson, J. H.; manuscript in preparation.
(5) (a) Champion, P. M.; Münck, E.; Debrunner, P. G.; Hollenberg, P. F.; Hager, L. P. *Biochemistry* **1973**, *12*, 426–435. (b) Hollenberg, P. F.; Hager, L. P. *J. Biol. Chem.* **1973**, *248*, 2630–2633. (c) Dawson, J. H.; Trudell, J. R.; Barth, G.; Linder, R. E.; Bunnenberg, E.; Djerassi, C.; Chiang, R.; Hager, L. P. *J. Am. Chem. Soc.* **1976**, *98*, 3709–3710. (d) Cramer, S. P.; Dawson, J. H.; Hodgson, K. O.; Hager, L. P. *J. Am. Chem. Soc.* **1978**, *100*, 7282–7290. (e) Sono, M.; Dawson, J. H.; Hager, L. P. *J. Biol. Chem.* **1984**, *259*, 13209–13216. (f) Sono, M.; Dawson, J. H.; Hager, L. P. *Inorg. Chem.* **1985**, *24*, 4339–4343. (g) Sono, M.; Dawson, J. H.; Hall, K.; Hager, L. P. *Biochemistry* **1986**, *24*, 347–356.
(6) Caron, C.; Mitschler, A.; Riviere, G.; Ricard, L.; Schappacher, M.; Weiss, R. *J. Am. Chem. Soc.* **1979**, *101*, 7401–7402.
(7) Ricard, L.; Schappacher, M.; Weiss, R.; Montiel-Montoya, R.; Bill, E.; Gonser, U.; Trautwein, A. *Nouv. J. Chim.* **1983**, *7*, 405–408.
(8) Mashiko, T.; Reed, C. A.; Haller, K. J.; Kastner, M. E.; Scheidt, W. R. *J. Am. Chem. Soc.* **1981**, *103*, 5758–5767.
(9) Jameson, G. B.; Robinson, W. T.; Collman, J. P.; Sorrell, T. N. *Inorg. Chem.* **1978**, *17*, 858–864.
(10) Berzinis, A. P.; Traylor, T. G. *Biochem. Biophys. Res. Commun.* **1979**, *87*, 229–235.
(11) Collman, J. P.; Sorrell, T. N. *J. Am. Chem. Soc.* **1975**, *97*, 4133–4144.
(12) (a) Cramer, S. P.; Hodgson, K. O. *Prog. Inorg. Chem.* **1979**, *25*, 1–39. (b) Penner-Hahn, J. E.; Hodgson, K. O. In *Iron Porphyrins, Part 3*; Lever, A. B. P., Gray, H. B., Eds.; VCH Publishers: Weinheim, West Germany; in press.

0020-1669/86/1325-4307$01.50/0